Adriano Aparecido Virgílio
Adriano Rogério Bruno Tech
Lilian Elgalise Techio Pereira

# ImageVI's

The software that collects the Vegetation Indices you need

# USER MANUAL

Pirassununga
Faculdade de Zootecnia e Engenharia de Alimentos
2020

Adriano Aparecido Virgílio
Adriano Rogério Bruno Tech
Lilian Elgalise Techio Pereira

# ImageVI's

The software that collects the Vegetation Indices you need

# USER MANUAL

DOI: 10.11606/9786587023007

**Graphic Design & Translation**:
Marilia M.G. Bastos

**Pirassununga**
**Faculdade de Zootecnia e Engenharia de Alimentos**
**2020**

**Faculdade de Zootecnia e Engenharia de Alimentos da**

**Universidade de São Paulo FZEA-USP**

Avenida Duque de Caxias Norte, 225

Pirassununga, SP

CEP 13635-900

http://www.fzea.usp.br



Dados Internacionais de Catalogação na Publicação
Serviço de Biblioteca e Informação da Faculdade de Zootecnia e Engenharia de Alimentos da Universidade de São Paulo

V816i

Virgílio, Adriano Aparecido
ImageVI's: the software that collects the vegetation indices you need: user manual. / Adriano Aparecido Virgílio, Adriano Rogério Bruno Tech, Lilian Elgalise Techio Pereira. - - Pirassununga: Faculdade de Zootecnia e Engenharia de Alimentos, 2020.
58 p.

ISBN 978-65-87023-00-7 (e-book)
DOI: 10.11606/9786587023007

1. Software development. 2. Image processing. 3. Vegetation index. 4. Digital image analysis. I. Tech, Adriano Rogério Bruno. II. Pereira, Lilian Elgalise Techio. Título.

Ficha catalográfica elaborada por Girlei Aparecido de Lima, CRB-8/7113

# PREFACE

The ImageVI's software was developed aiming at to make easier the extraction of vegetation indices (VI's) from images acquired in the field or in a controlled environment.

The VI's calculated and provided by the software are derived from the RGB (red, green, blue) and HSB (Hue, Saturation and Brigthness) color systems. The images can be composed of either samples containing multiple or individual leaves, being applied to the most diverse of plant species.

The software is capable of processing images with a white background, acquired with commercial cameras, scanners, cellphone cameras, smartphones or tablets, as long as the lighting conditions do not have excessive noise (reflections, shadows, dirt in the background, etc.).

This manual contains the software's basic information, but it also provides tips and important information about the standardization of image acquisition procedures, pointing out common mistakes to avoid in this step.

We hope that the software can be used as practical tool, easily accessible and widely used for extracting VI's in vegetation studies, providing fast results for your research or studies.

The authors

The most beautiful gift of nature is that it gives one pleasure to look around and try to comprehend what we see.

Albert Einstein

# INDEX

# 1. A brief history of photography

The earliest optical inventions date back at least to the ancient Greek era. Long before the photographs were made, the first to discover and develop the scientific principles of optics was the Mohist Chinese Philosopher Mo Di (470 B.C.-391 B.C.), by observing the natural optical phenomenon that occurs when an image is projected through a small hole on a surface opposite to the opening, producing an inverted image. Afterwards, Greek mathematicians Aristotle and Euclid, as well as the Byzantine mathematician Anthemius of Tralles, applied the same principles to develop their experiments.

For the image to be clear it would be necessary that sourroudings be relatively dark, so many historical experiments were performed in dark rooms. The principle is known as **pinhole image**, and the device was called "camera obscura", due to the use of devices that make use of the principle within a box, tent, or room. Many scientists experimented with a small hole and light but none of them suggested that a screen is used so an image from one side of a hole in surface could be projected at the screen on the other.

First one to do was Alhazen (also known as Ibn al-Haytham) in 11th century. The techniques described in Ibn al-Haytham's Book of Optics are capable of producing primitive photographs using medieval materials (Figure 1).

**Figure 1.** Obscura, the Ancient Camera. Obscura is a Latin word means Darkroom.

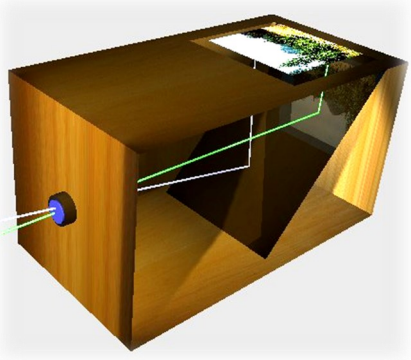

To find more informations, please access
https://www.misterlocation.com/blog/history-of-studio-photography/

Souce: https://simple.wikipedia.org/wiki/Camera_obscura#/media/File:Camera_obscura_box.jpg

# 1. A brief history of photography

Heliography, the world's first known photographic process, was invented by Nicéphore Niépce around 1824. After Niépce's death in 1833, Louis-Jacques-Mandé Daguerre invented one of early photography's most important technologies, the Daguerreotype. This new artform, which was officially invented between 1838 and 1840, followed the same principles as Heliography. The next few years were an exciting time for advancements in the science of photography and finally in 1841, Hippolyte Fizeau invented short focal lenses, allowing exposure times to drop from 30 minutes to just a few seconds. With the use of the first cameras for recording landscapes, people and objects, the photography had passed for crescent evolutive processes between 1839 and 1900 (Figure 2). Since then, its objective is precisely to stop time and allow memories or episodes to be recorded for the posterity, being widely used all over the world.

**Figure 2.** A brief history of photography and the camera. Illustration: Vin Ganapathy. © The Spruce, 2018.

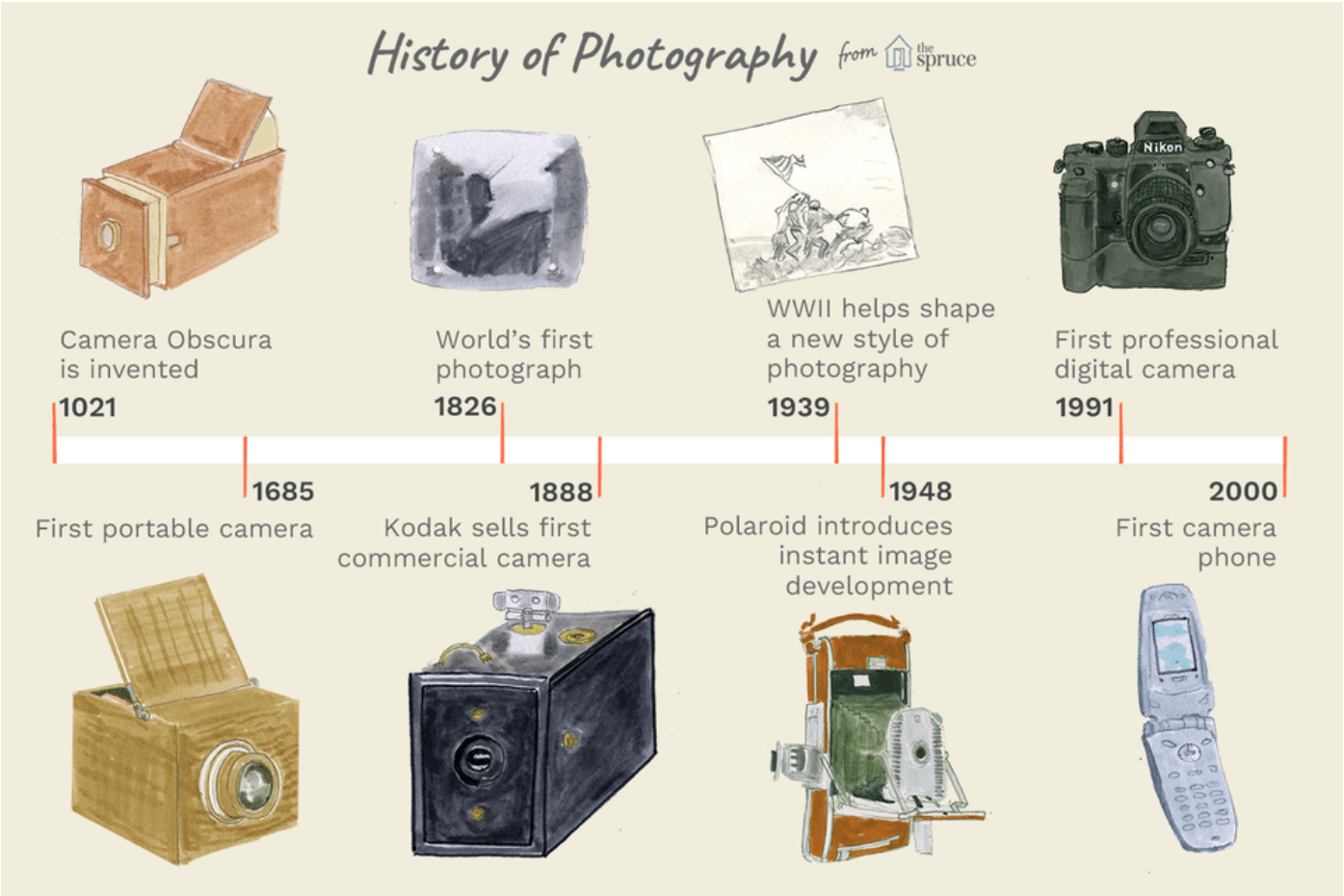


Source: Masoner (2020).

# 2. Basic steps of the digital image processing

Every image can hold much more than a simple memory, since is capable of save and store details about a certain object, person, animal or even a plant, bringing relevant information that can help us to understand situations that often go unnoticed. Thus, we can understand an image as being a source of information even without direct contact with the person who takes the photo or with the photographed object.

From this point of view, image processing methods had evolved, and stems from two principal application: improvement of pictorial information for human interpretation, and processing of scene data for autonomous machine perception. The image analysis and computer vision aim to replicate and improve the effect of human vision by electronically or digitally, perceiving, understanding and interpreting them in a digital image processing system. The image processing methods are applied for enhancement or other manipulation of the image, meanwhile the computer vision systems provide the analysis of its content. Basically, there are three levels in digital image processing, low, mid and high-level processes (Figure 3). In the low-level of processing basic operations are used to obtain a higher quality image or highlights specific objects, such as noise reduction, contrast enhancement, etc. Mid-level processing is applied when we aim to extract image atributes, using tasks such as object recognition or classification. The high-level processing normally is associated with computer vision, since the inputs of the processes are the image's attributes and the outputs are used to understanding, make sense of an ensemble of recognized objects or to perform cognitive functions.

**Figure 3.** Levels of processing in digital image processing.

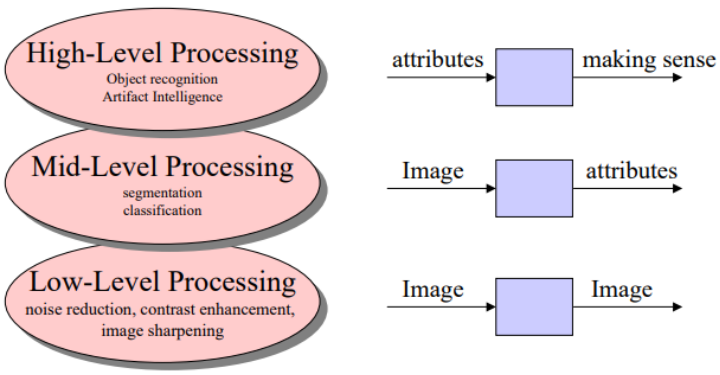


Source: Gonzalez and Woods (2008).

# 2. Basic steps of the digital image processing

For a point of view of digital image analysis the first action required is to acquire or **(1) capturing the image**. The image is captured by a sensor (eg. Camera), and digitized if the output of the camera or sensor is not already in digital form, using analogue-to-digital convertor. In this step, the image acquired is completely unprocessed. According to Annadurai and Shanmugalakshmi (2007, p.9):

> *"the digitizer is nothing but an analog to digital converter to convert the electrical sign corresponding to the intensities of the optical image into a digital image. There may be one or more frame buffers for fast access to image data during processing."*

The second step in this process is related to **(2) Image enhancement**, and the idea behind enhancement techniques is to bring out details that are hidden, or simple to highlight certain features of interest in an image. It usually includes sharpening of images, brightness and contrast adjustments, noise removal and/or others.

The **(3) image restoration** is an area that also deals with improving the appearance of an image. However, meanwhile enhancement is subjective, image restoration is more objective, because restoration techniques are based on mathematical or probabilistic models of image degradation.

**(4) Color image processing** use the colour of the image to extract features of interest and may include color modeling, such as RGB or HSB color models (next chapter), and processing in a digital domain.

**(5) Wavelets and Multiresolution Processing** are the foundation of representing images in various degrees of resolution, being used for image data **(6) compression**, as images follows up subdivision successively into smaller regions for data compression and for pyramidal representation. Compression deals with techniques for reducing the storage required to save an image or the bandwidth to transmit it, and its use for displaying images on the internet it is very much necessary to compress data and also increases the loading speed of websites.

# 2. Basic steps of the digital image processing

Tools for extracting image components that are useful in the representation and description of shape, including morphological operations like erosion and dilation are in the **(7) morphological processing** steps. In this step, there would be a transition from processes that output images to processes that output image attributes. The following steps **(8) segmentation, (9) representation and description and (10) object recognition** are processes which output the attributes of the image.

**Figure 4.** Fundamental steps on digital image processing.

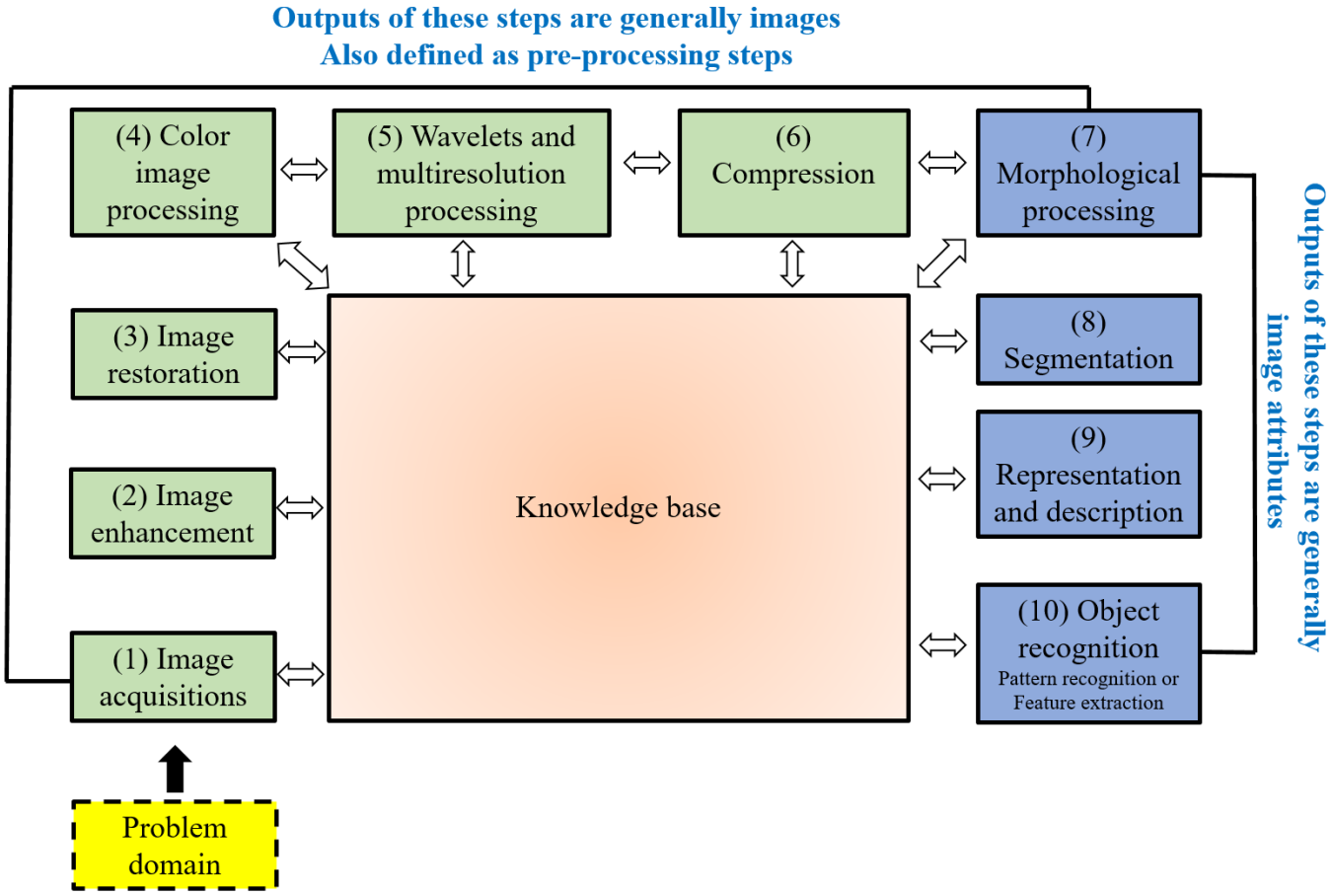


Adapted from Gonzalez and Woods (2008). **Digital image processing.** 3 ed. Prentice Hall.

In general, autonomous segmentation is one of the most difficult tasks in digital image processing. A rugged segmentation procedure brings the process a long way toward successful solution of imaging problems that require objects to be identified individually. Then, the more accurate the segmentation, the more likely recognition is to succeed.

# 2. Basic steps of the digital image processing

Segmentation algorithms generally are based on one or two properties of intensity values, such as discontinuity (of point, lines or edges for which the most common way is to run a mask through the image) and similarity, which are made employing thresholding methods, the first step in any segmentation approach. Representation and description almost always follow the output of a segmentation stage, which usually is raw pixel data, constituting either the boundary of a region or all the points in the region itself. Choosing a representation is only part of the solution for transforming raw data into a form suitable for subsequent computer processing (mainly recognition). Representation can be made by determining a subset of the initial features, called **feature selection**, and this procedure can be made by using principal component analysis, which is considered a simpler feature extraction technique. The selected features are expected to contain the relevant information from the input data, so that the desired task can be performed by using this reduced representation instead of the complete initial data. Description then deals with extracting attributes that result in some quantitative information of interest or are basic for differentiating one class of objects from another.

In machine learning, pattern recognition or object recognition, and in image processing the feature extraction, starts from an initial set of measured data and builds derived values (features) intended to be informative and non-redundant, facilitating the subsequent learning and generalization steps and, in some cases, leading to better human interpretations. The central aim of the pattern recognition step is the concept of 'learning' from sample patterns. According to Gonzalez and Woods (2008, p. 883):

> *"...a pattern is an arrangement of descriptors (feature), and a pattern class is a family of patterns that share common properties. Pattern recognition by machine involves techniques for assigning patterns to their respective classes - automatically and with as little human intervention as possible."*

Pattern recognition algorithms generally aim to provide a reasonable answer for all possible inputs and to perform "most likely" matching of the inputs, taking into account their statistical variation.

# 3. RGB and HSB color systems

**The RGB color model** is an additive color system that combines red, green and blue lights to create the colors we see. The main purpose of the RGB color model is to detect, represent and display images in electronic systems, such as televisions and computers, but it has also been used in conventional photography and cell phone cameras. RGB is an additive color system because it combines its primary colors creating the many colors we perceive, stimulating the different types of conical cells (photoreceptors) simultaneously.

A color in the RGB color model can be described indicating how much of each wavelength the spectrum of red, green and blue is included. In digital images, the image is composed of pixels or image elements, which is the smallest unit of the image, being represented by a matrix, where each matrix represents a spectrum of the electromagnetic field, that is, a color in gray intensities. Each pixel carries information, or values, that represent the three colors of the additive model, red, green and blue (RGB). The possibilities of mixing the three primary colors together can be represented as a three-dimensional coordinate plane with the values for R (red), G (green) and B (blue) on each axis. This coordinate plane produces a cube called the RGB color space (Figure 5). The color is expressed as an RGB triplet (r, g, b), whose component can vary from zero (less saturated) to 255 (more saturated). If all components are zero, the result will be black; if all are at maximum, the result will be the brightest representable white.

**Figure 5.** Diagram representing the RGB cubic model.

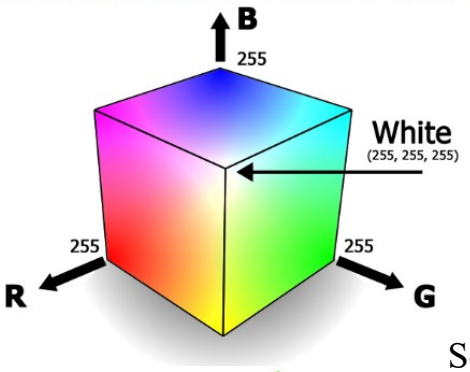


Source: Cunha (2020).

# 3. RGB and HSB color systems

The color of the pixel is then characterized by a three dimensional space (Red, Green, Blue) being represented by the combination of three values, ranging from 0 to 255 and the interpolation of these three values results in an unique color in each pixel. The main application of the RGB color model is to display digital images. Each pixel on these displays is built by using three small and very close RGB light sources. At a common viewing distance, these colors cannot be distinguished separately and are viewed as a single solid color. Digital cameras for photography that use a CMOS or CCD image sensor mostly perform with some type of RGB color model.

However, it is important to notice that the same art displayed on a computer monitor may not match to that printed in a publication. This is because in the printing industry it is used the CMYK Colour System – Cyan, Magenta, Yellow and Black, and colours are created using physical pigments. In both CMYK and RGB models we end up seeing the colours that reflect from the object to the human eye. RGB colours are more intense than CMYK (Figure 6).

Dekel, G. RGB and CMYK Colour systems. Available in: http://www.poeticmind.co.uk/research/rgb-cmyk-colour-systems/

**Figure 6.** The RGB and CMYK diferences of a digital image.


Source: https://blog.expanssiva.com.br/as-diferencas-de-cmyk-x-rgb/

# 3. RGB and HSB color systems

Screen colours are created electronically using projected light, which is more vivid than light that bounces off dyes printed on paper. Inks also tend to be absorbed (spread) in the paper and lose their intensity. Thus the best design method is to design in RGB and convert to CMYK as close to the printing stage as possible. If you are working on a design that starts in Photoshop, goes through InDesign and finally prints from a PDF, then convert to CMYK while PDFing.

The **HSV or HSB model** is color system formed by the combination of hue, saturation and value or brightness, respectively. This color space describes colors (hue or tint) in terms of their shade (saturation or amount of gray) and their brightness value. This system was developed in 1978, being a non-linear transformation of the RGB system, and the representation of the colors is closer to how humans perceive them.

The Hue or matrix is the pure color with maximum values of saturation and luminosity (orange, red, green, ...). This parameter can varies from 0 to 360º, being most common to use its normalized values, varying from 0 to 100%. Since each color is situated in a different degree, this attribute makes it possible to distinguish the various pure colors with a different degree (Figure 7).

**Figure 7.** Diagram representing the HSV or HSB color space.

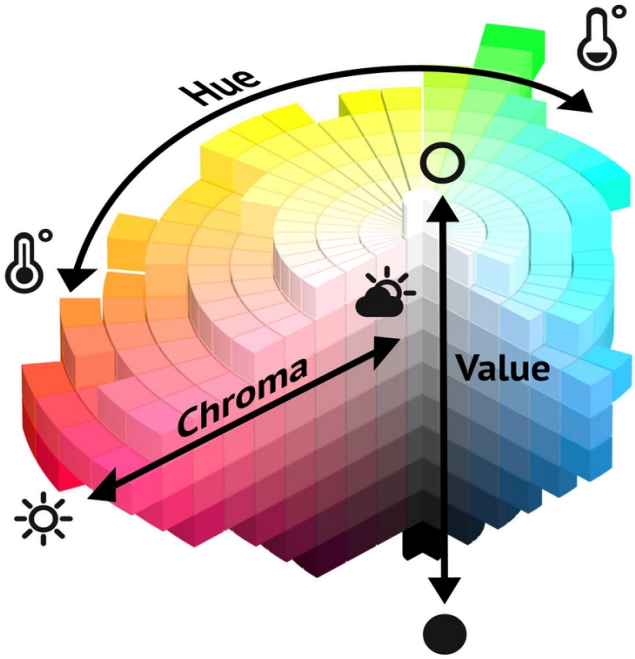


Source: https://www.subpng.com/png-b2601i/download.html

Bear, J. H. (2019). The HSV Color Model in Graphic Design. Available in https://www.lifewire.com/what-is-hsv-in-design-1078068

# 3. RGB and HSB color systems

Saturation or chroma describes the amount of gray in a particular color, from 0 to 100 percent. Reducing this component toward zero introduces more gray and produces a faded effect. Sometimes, saturation appears as a range from just 0-1, where 0 is gray, and 1 is a primary color.

Value or brightness works in conjunction with saturation (chroma) and describes the brightness or intensity of the color, also varying from 0-100%, where 0 is completely black, and 100% is the brightest and reveals the most color. In other words, the closer the value is to 100%, the lighter the color, while the closer the value is to 0% the darker the color.

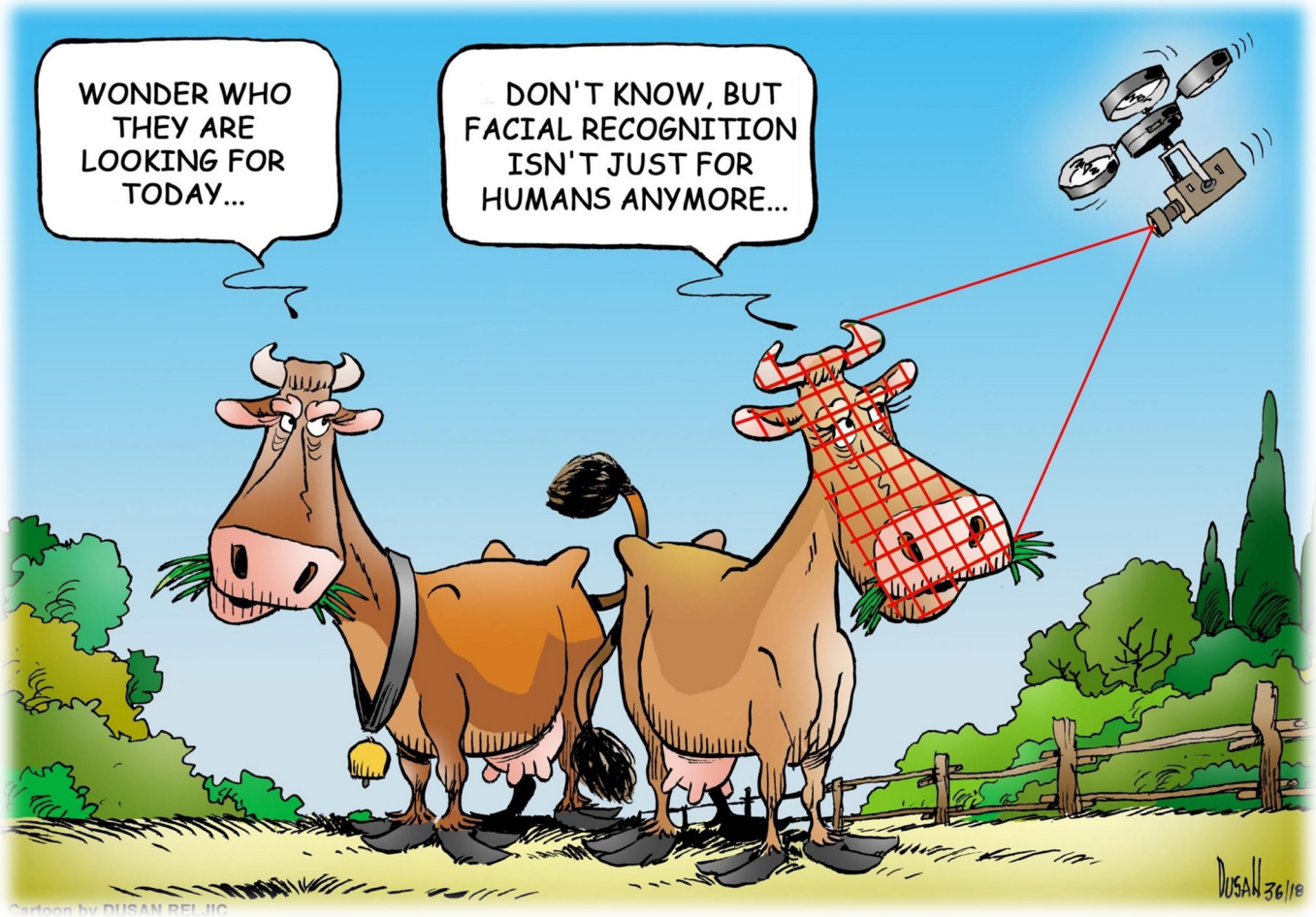


Souce: Reljic (2020)

# 4. Using digital image processing for plant analysis

According to Barbosa et al. (2016), plant visual analysis is performed empirically by man since the dawn of agriculture. Currently, the advent of digital cameras has provided an essential evaluation tool from images. The analysis of plants through images has been held in all plant organs, on scales ranging from micro to macroscopic and in diverse environments. Color image processing procedures have been mostly used in agriculture for adjusting the field practices like fertilizer and pesticide application according to demands and for maximizing agricultural profit (El-Azazy, 2018).

For these purposes, it is assumed that the quantification of physiological or morphological processes in plant components, i.e., leaves, stem segments, flowers, fruits, etc., may show differential behavior as a function of environmental stress, and result in different leaf-level photosynthetic activity, carbohydrate content in a plant segment or nutrientes content. These processes can be captured by an image due to the wavelenghts reflected, absorbed or tramsmitted by the plant parts (Figure 8).

**Figure 8.** Mapping photosynthesis from Space - a new vegetation-fluorescence technique.

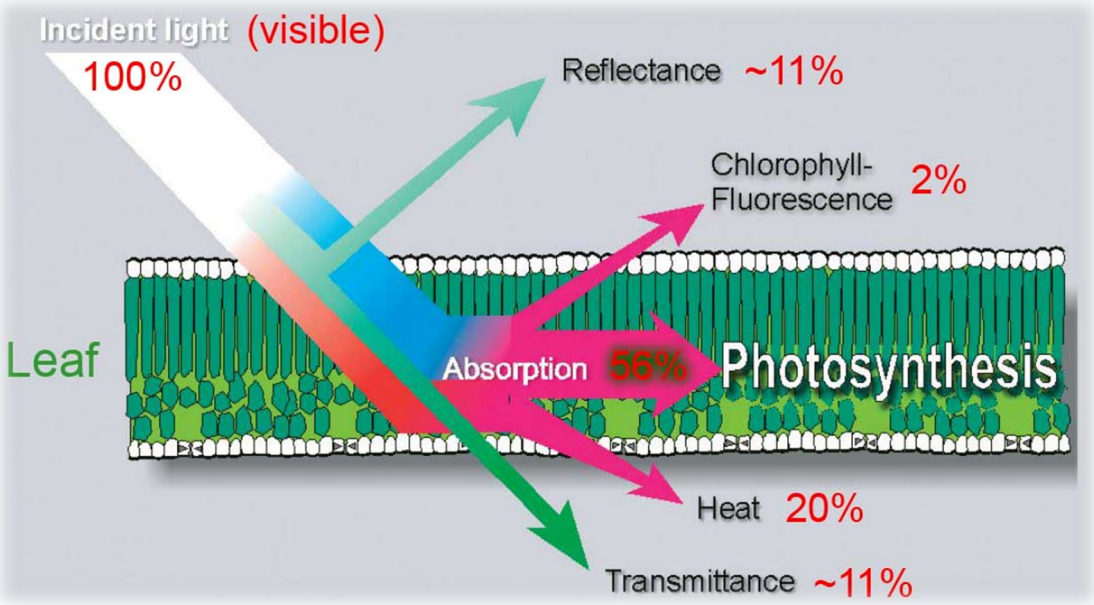


Source: Davidson et al. (2003).

# 4. Using digital image processing for plant analysis

In the nature, the light performs major functions in plant growth and development. It is essential in the production of energy through the process of photosynthesis, but also influences or controls other plant growth processes such as the synthesis of the photoreceptors (e.g. chlorophyll, other pigments), photomorphogenesis (organ formation and development), phototropism (plant response to unilateral light), photoperiodism, translocation, mineral absorption, and transpiration.

https://www.cropsreview.com/what-is-light.html

Light is a form of electromagnetic radiation, a type of energy that travels in waves. Every electromagnetic wave has a particular wavelength, or distance from one crest to the next, and different types of radiation have different characteristic ranges of wavelengths. The visible spectrum is the only part of the electromagnetic spectrum that can be seen by the human eye. It includes electromagnetic radiation whose wavelength is between about 400 nm and 700 nm (Figure 9). Visible light from the sun appears white, but it's actually made up of multiple wavelengths (colors) of light.

**Figure 9.** The light spectrum.

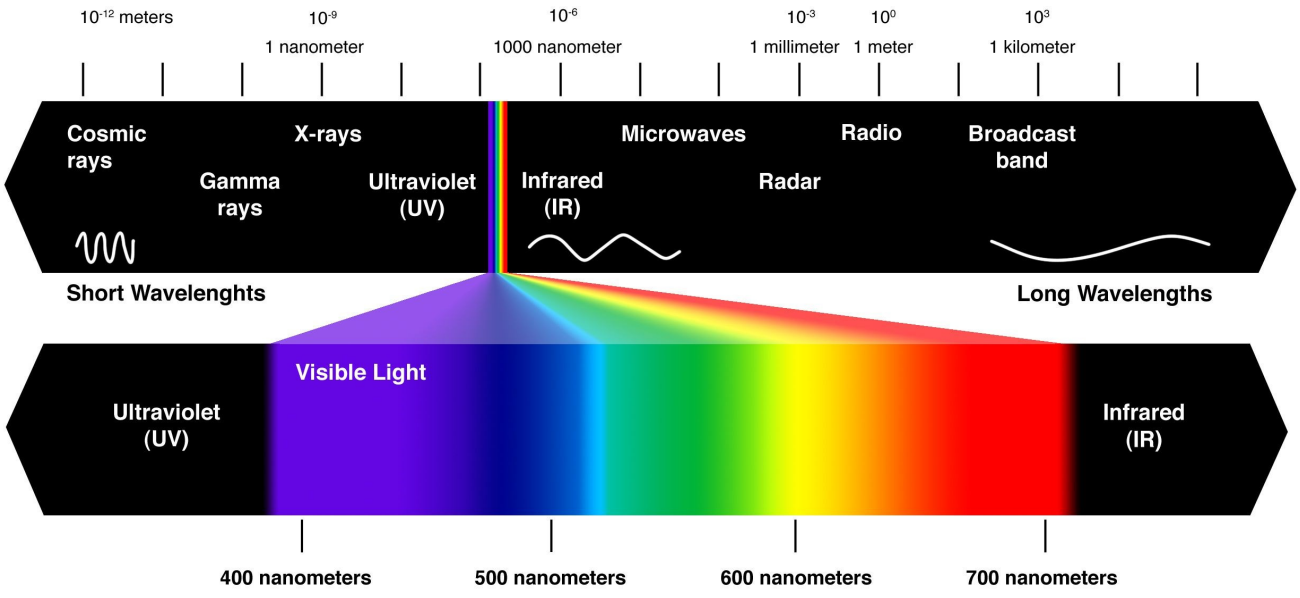


Source: https://ledgrowlightsguides.com/full-spectrum-led-grow-light/

# 4. Using digital image processing for plant analysis

In photosynthesis, the sun's energy is converted to chemical energy by photosynthetic organisms. However, the various wavelengths in sunlight are not all used equally in photosynthesis. Instead, photosynthetic organisms contain light-absorbing molecules called pigments that absorb only specific wavelengths of visible light, while reflecting others. The set of wavelengths absorbed by a pigment is its absorption spectrum (Figure 10), and there are three key pigments in photosynthesis: chlorophyll a, chlorophyll b, and β-carotene. The set of wavelengths that a pigment doesn't absorb are reflected, and the reflected light is what we see as color.

**Figure 10.** Spectrum of absorption of photosynthetic pigments.

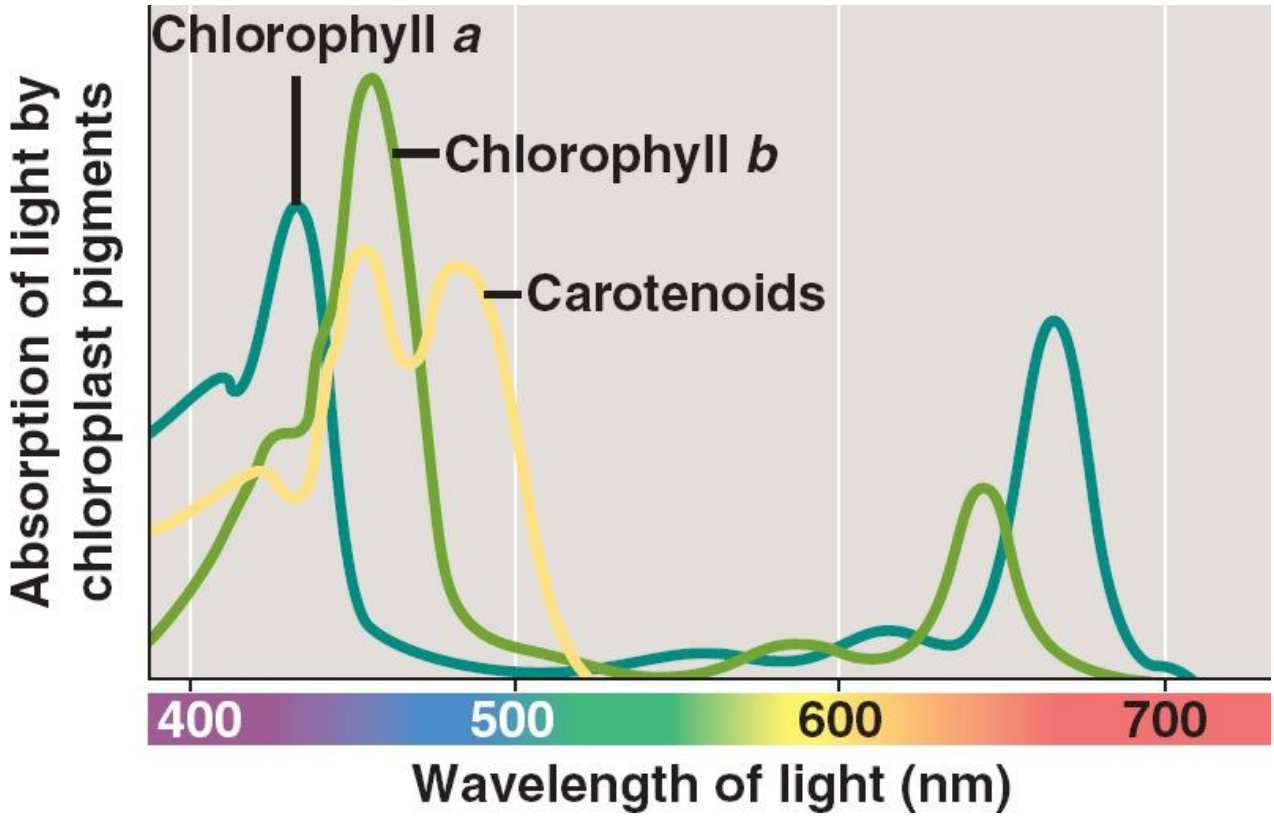


Source: https://socratic.org/questions/how-does-light-frequency-affect-the-rate-of-photosynthesis

Text extracted from: **Light and photosynthetic pigments.** Available in: https://www.khanacademy.org/science/biology/photosynthesis-in-plants/the-light-dependent-reactions-of-photosynthesis/a/light-and-photosynthetic-pigments

# 4. Using digital image processing for plant analysis

Chlorophyll molecules absorb blue and red wavelengths. Carotenoids also help to capture light, but they also have an important role in getting rid of excess light energy. When a leaf is exposed to full sun, it receives a huge amount of energy (Figure 11); if that energy is not handled properly, it can damage the photosynthetic machinery. Carotenoids in chloroplasts help absorb the excess energy and dissipate it as heat. The, carotenoids are another key group of pigments that absorb violet and blue-green light.

Text extracted from: **Light and photosynthetic pigments.** Available in: https://www.khanacademy.org/science/biology/photosynthesis-in-plants/the-light-dependent-reactions-of-photosynthesis/a/light-and-photosynthetic-pigments

Thus, in the visible region (red, green and blue wavelengths), leaf reflectance is dictated by the amount and concentration of photosynthetic pigments, including chlorophyll, xanthophylls, anthocyanins and carotenoids (Sims and Gamon, 2002). These pigments, when in high concentration in the leaf, strongly absorb the wavelengths of the solar radiation in the blue (400 – 495 nm) and red edge (650 – 699 nm) regions. Chlorophyll and carotenoid concentration account for around 67.7% of the variability in reflectance of the green (550 nm) wavelenghts (Buscaglia and Varco, 2002).

**Figure 11.** Different patterns of leaf reflectance.

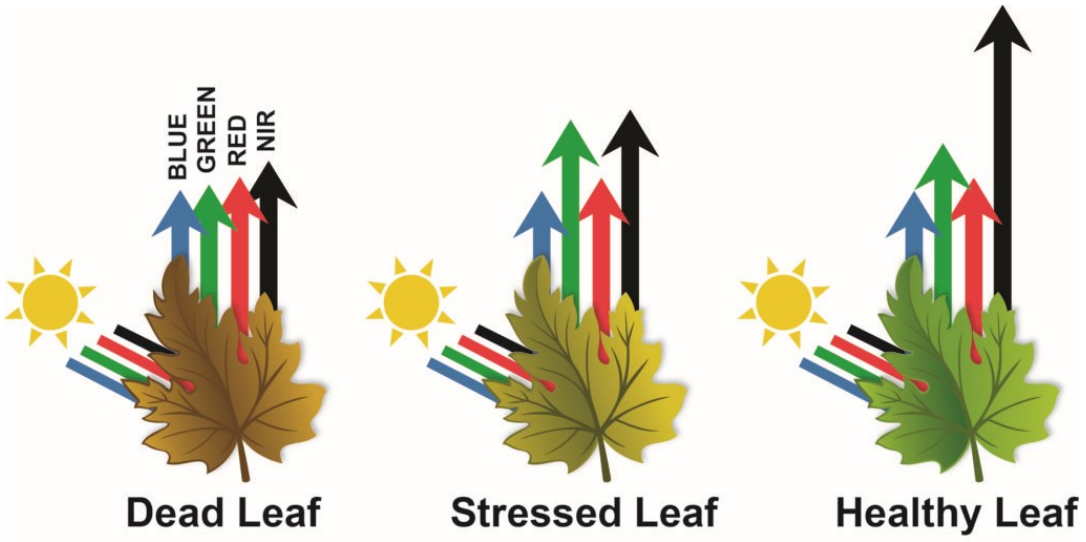


Source: https://midopt.com/healthy-crop/

# 4. Using digital image processing for plant analysis

Remote sensing techniques based on image analysis relyes on the principle that the relationship between spectral reflectance of leaves or canopy at various wavelengths is accurately correlated with canopy growth traits, plant nutrients status and productivity (Wang et al., 2014), and that such relationships can be described by exploring information contained in images. For example, N deficiency reduces leaf chlorophyll unmasking the yellow or brown color of carotenoid pigments (isomeric forms of carotenes and xanthophylls) within leaves. This results in less leaf absorption in the blue and red bands, giving the stressed vegetation a yellowish or brownish color.

Overall research results indicate that plant nutritional status can be detected by analyzing RGB components of images (Figure 12), with a potential for becoming a decision support tool for fertilizer application and timely correction of nutrient deficiency before irreversible growth impact occurs (Sridevy et al., 2018).

**Figure 12.** Schematic figure representing variations in RGB values of the images according to the plant nitrogen (N) content.


| RGB color | Values |
|---|---|
| R | 132 |
| G | 153 |
| B | 123 |
| $R_N$ | 0.32 |
| $G_N$ | 0.37 |
| $B_N$ | 0.30 |

| RGB color | Values |
|---|---|
| R | 142 |
| G | 166 |
| B | 109 |
| $R_N$ | 0.34 |
| $G_N$ | 0.40 |
| $B_N$ | 0.26 |

| RGB color | Values |
|---|---|
| R | 159 |
| G | 185 |
| B | 112 |
| $R_N$ | 0.35 |
| $G_N$ | 0.41 |
| $B_N$ | 0.25 |

Source: Mancin (2020)

# 4. Using digital image processing for plant analysis

Remember that the RGB individual values represent intensities of the primary color components in a gray scale, each varying from 255 (a pure white color) to 0 (zero is the pure black color). Thus, the higher the value of the green and red components of an image, the closer to the pure white color (255, 255, 255), and consequently lower greenness is detected, indicating lower leaf N content (Figure 13). The blue component has been less variable across gradients of N contents or leaf pigments content in several species.

Mata-Donjuan et al. (2012) highlighted that the RGB color space was not originally conceived for image processing but it was designed for computer graphics and, as a result, the RGB color space is very susceptible to light conditions during image acquisition procedures. According to Karcher and Richardson (2003), the intensity of red and blue can change the perception of greenness in a given image. In view of this, the HSB color space is normally used in a complementary way with the RGB color space in order to analyze possible effects of light conditions in the images acquired.

**Figure 13.** Diagram representing variations in RGB values according to the plant nitrogen (N) content.

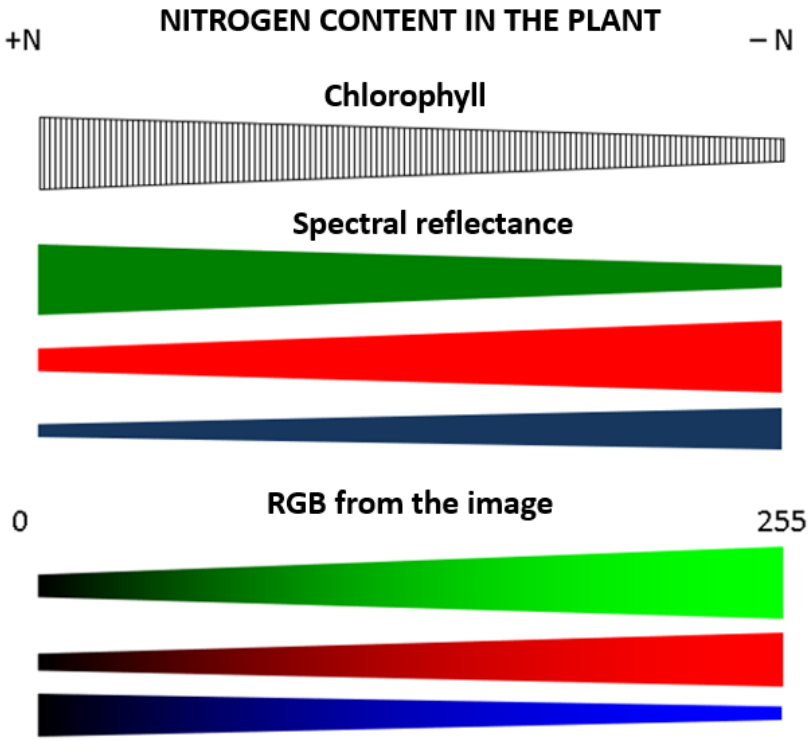


Source: Mancin (2020)

# 5. Vegetation indices and image analysis

The vegetation indices (VI´s) are mathematical measures developed to measure, in a quantitative way, individual spectral bands of the vegetation. They can be based on the reflectance of vegetation in the visible spectral region, that represents the absorption and reflection of the wavelenghts of solar radiation by the action of photosynthetic pigments located inside the leaves (Ponzoni, Shimabukuro and Kuplich, 2012). Their values are used to help in the interpretation of the information obtained from digital images (Bannari et al., 1995). According to Gitelson (2013), many algorithms have been developed for the remote estimation of vegetation fraction in terms of combinations of spectral bands, derivatives of reflectance spectra, neural networks, inversion of radiative transfer models, and several multispectral statistical approaches. The most widespread type of algorithm used is the mathematical combination of visible and near-infrared reflectance, in the form of spectral vegetation indices.

Besides the RGB values, the software ImageVI's automatically calculates the following VI's:

**Normalized red channel (RN):** The RN (also described by the lower case 'r') vegetation index corresponds to the percentage of red reflectance in the total visible spectrum (RGB). This index is calculated through the equation R / (R + G + B) ranging from 0 to 1.

**Normalized green channel (GN):** The GN vegetation index (also described by the lower case 'g'), corresponds to the percentage of reflectance of green in the total visible spectrum (RGB). The index is calculated using the equation G / (R + G + B) ranging from 0 to 1.

**Normalized blue channel (BN):** The BN vegetation index (also described by the lower case 'b'), corresponds to the percentage of blue reflectance in the visible spectrum (RGB). This index is calculated using the equation B / (R + G + B) in the range 0 to 1.

# 5. Vegetation indices and image analysis

**Hue (H):** is the result of an equation that transforms the RGB color system in the HSV or HSB color space. "Hue" differs slightly from "color" because a color can have saturation or brightness as well as a hue. Hue is more specifically described by the dominant wavelength (Figure 13), and it is also a term which describes a dimension of color we readily experience when we look at color, or its purest form. When discussing spectral "light primaries" (RGB), a pure hue equivalent to full saturation is determined by the ratio of the dominant wavelength to other wavelengths in the color.

$$H = \begin{cases} 60 \times \frac{G-B}{MAX-MIN} + 0, & \text{if } MAX = R \text{ and } G \geq B \\ 60 \times \frac{G-B}{MAX-MIN} + 360, & \text{if } MAX = R \text{ and } G < B \\ 60 \times \frac{B-R}{MAX-MIN} + 120, & \text{if } MAX = G \\ 60 \times \frac{R-G}{MAX-MIN} + 240, & \text{if } MAX = B \end{cases}$$

**Saturation (S):** defines the brilliance and intensity of a color. Saturation refers to how pure or intense a given hue is. 100% saturation means there's no addition of gray to the hue. The color is completely pure. The more saturated (closer to 100%) a color is, the more vivid or brighter it appears. At the other extreme a hue with 0% saturation appears as a medium gray. It is used to calculate the DGCI vegetation index (Dark Green Color Index).

$$S = \frac{MAX - MIN}{MAX}$$

**Figure 13.** Diagram representing HSV model with full range of a single hue.

**Value or Brightness (V or B):**
In terms of a spectral definition of color, value describes the overall intensity or strength of the light. Both S and B are measured from 0 to 100% or from 0 to 1.

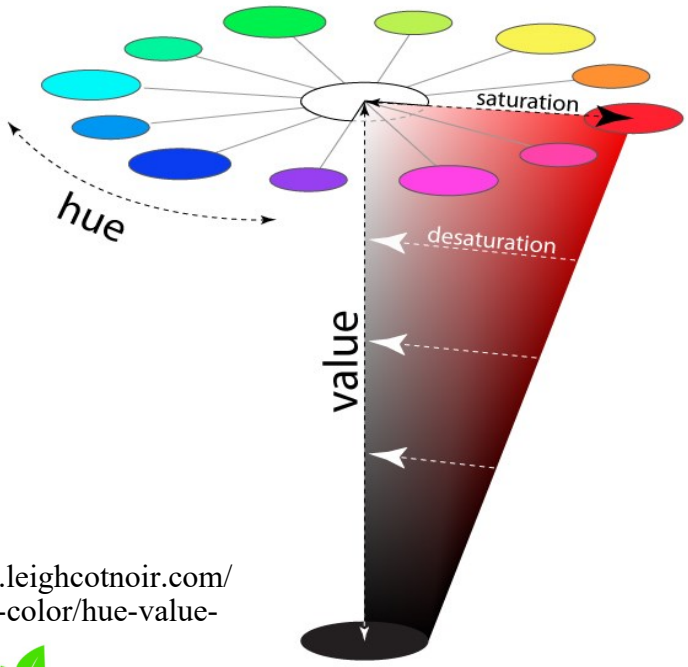


Source: http://learn.leighcotnoir.com/artspeak/elements-color/hue-value-

# 5. Vegetation indices and image analysis

**VARIgreen (Visible Atmospherically Resistant Index):** The VARIgreen vegetation index was proposed by Gitelson et al (2002) aiming at to correct atmospheric effects on the canopy. Spectral indices were based only on bands in the visible spectrum: the green (near 550 nm) or red edge near 700 nm, and the red (near 670 nm), as means of measuring a canopy biophysical properties defined as vegetation fraction (VF). According to the authors, the VIgreen= (Green - Red/Green + Red) is sensitive to canopy VF, but the effect of the atmosphere on the red and green is similar since both are adjacent in the spectrum. Although the green has a shorter wavelength, green reflectance is higher, so the two effects (numerator and denominator) cancel each other. The atmospheric effects exist in the green and red of the denominator of VI index. Other indices, such as ARVI, is assumed that the effect in the blue is twice as large as in the red, so to correct for the effect in the red and the green, it was subtracted blue reflectance. In this way, VARIgreen was designed to introduce an atmospheric self-correction. It was observed that VARIgreen had a more linear relationship with VF than VIgreen, and was 32% more sensitive to VF. In a general way, this index have a high correlation with leaf area index and dry matter yield than with parameters related with nitrogen nutrition.

**DGCI (Dark Green Color Index):** To simplify the interpretation of digital color data from RGB models to a more more intuitive color model based on hue, saturation, and brightness (HSB, considering an human perception of color) Karcher and Richardson (2003), working with quality of turfgrass in response to N fertilizer, processed HSB values into a single measure defined as dark green color index (DGCI). Across all turf varieties and N treatments, authors observed that DGCI values were a more consistent measure of green color than individual RGB values. Rorie et al (2011) detected that the response of DGCI to leaf N concentration in corn reached a plateau and could no longer differentiate nitrogen concentration above a given value (it will be species-specific). In addition, differences in lighting conditions could be eliminated by measuring with the same camera under full illumination between 1300 and 1500 h, and, the inclusion of disks of known color to correct images largely eliminated variation due to camera and lighting conditions.

# 5. Vegetation indices and image analysis

**Excess of green (ExG):** Originally described by Woebbecke et al. (1995), the ExG provided a near-binary intensity image outlining a plant region of interest, being able to distinguished weeds from a nonplant background. The plant regions of interest were then binarized using a selected threshold value for each set of images.

**Excess of red (ExR):** Meyer et al. (1998) considered that there are 4% blue, and 32% green, compared with 64% red cones in the retina of the human eye to introduced ExR method to segment leaf regions from the background. ExR was able to separate the plant pixels from background pixels, but it was not as accurate as ExG. The original index was calculated as ExR = 1.3r - g, but in Guijarro et al (2011) it was used ExR = 1.4r - g. Authors described that because the soil is a relevant part in the crop fields, it would be of interest to retain the greatest number of pixels that are potential candidates as textures in the soil. Then, the goal of detecting redness is to achieve their binarization, taking into account that it is associated to the textures belonging to the soil.

**Excess green minus excess red (ExGR):** Meyer and Camargo Neto (2008) approach used the 'excess green minus excess red index' for green VF estimation, by distinguish green plants against a natural background of soils and residues. As reported by the authors the soybean plants and grassy weeds were separated quite successfully from the background, and the index identified plant regions in full sun with accuracy of $0.88 \pm 0.06$, considering also that dry or wet canopy and soil surfaces had little impact on separation performance.

**Modified excess of green (MExG):** To discriminate vegetation pixels, a linear combination of the RGB planes with coefficients ($r = -0.884$, $g = 1.262$, $b = -0.311$) was performed by Burgos-Artizzu et al. (2011). These coefficients were found using a genetic algorithm optimization, and according to the authors they perform better than Excess Green coefficients ($r = -1$, $g = 2$, $b = -1$) (Woebbecke et al., 1995), on similar images. The discrimination between plant and soil region was effective because the MExG method was very robust to the changing illumination conditions.

# 5. Vegetation indices and image analysis

**Color Index of Vegetation Extraction (CIVE):** It was based on the principal component analysis of the information contained in the RGB bands by Kataoka et al. (2003) aiming at to separate the green plant portion from the background, and a discriminant analysis was used to determine the threshold level. Kataoka et al. found that the CIVE had better plant segmentation than Near-infrared (NIR) method because it provides greater emphasis of the green areas. In Beniaich et al. (2019), the indices CIVE and EXG presented a better performance in the vegetation classification during the cycles of jack bean and millet, according to the overall accuracy and Kappa coefficient.

$$CIVE = 0.441r - 0.881g + 0.385b + 18.78745$$

**Vegetative index (VEG):** Based on the physical study of the image of Beniaich et al. (2019), where 'a' is a constant with a reference value of 0.667.

$$VEG = \frac{g}{r^a b^{(1-a)}}$$

**Combined index (COM):** Guijarro et al. (2011) pointed out that in the set of images analyzed, methods based on ExG, CIVE, ExGR and VEG produce over-segmentation (excessive green is extracted) or under-segmentation (little green) depending on the images, and normally not all simultaneously in the same sense. Then, using different results obtained in studies, authors proposed to fuse them in a combined index.

$$COM = 0.25ExG + 0.3EXGR + 0.33CIVE + 0.12VEG$$

# 5. Vegetation indices and image analysis

The software ImageVI's automatically calculates the following VI's:

| VI's | Formula | Reference |
|---|---|---|
| $R_N$ | R/(R+G+B) | Yang *et al.* (2015) |
| $G_N$ | G/(R+G+B) | Yang *et al.* (2015) |
| $B_N$ | B/(R+G+B) | Yang *et al.* (2015) |
| H | $H = \begin{cases} 60 * \{(G-B)/[\max(RGB) - \min(RGB)]\}, \max(RGB) = R \\ 60 * \{2 + \{(B-R)/[\max(RGB) - \min(RGB)]\}\}, \max(RGB) = G \\ 60 * \{4 + \{(R-G)/[\max(RGB) - \min(RGB)]\}\}, \max(RGB) = B \end{cases}$ | Wang *et al.* (2014)<br>Yuan (2016) |
| S | Maximum(RGB)-Minimum(RGB)/Maximum(RGB) | Wang *et al.* (2014)<br>Yuan (2016) |
| V or B | Maximum(RGB)/255 | Wang *et al.* (2014)<br>Yuan (2016) |
| $VARI_{green}$ | VARI*green* = (G-R)/(G+R-B) | Gitelson *et al.* (2002) |
| DGCI | DGCI = [(Hue − 60)/60 + (1 − Saturation) + (1 − Brightness)]/3 | Saberioon *et al.*(2014)<br>Rorie *et al.* (2011)<br>Karcher e Richardson (2003) |
| ExG | $ExG = (2*G_N) - R_N - B_N$ | Guijarro *et al.* (2011)<br>Yang *et al.* (2015) |
| ExR | $ExR = (1.4*R_N) - G_N$ | Guijarro *et al.* (2011)<br>Meyer et al. (1998) |
| ExGR | ExGR = ExG – ExR | Guijarro *et al.* (2011)<br>Yang *et al.* (2015) |
| MExG | MExG= 1.262*G - 0.884*R - 0.311*B | Burgos-Artizzu *et al.* (2011) |
| CIVE | $CIVE = 0.441R_N - 0.811G_N + 0.385B_N + 18.78745$ | Guijarro *et al.* (2011)<br>Yang et al. (2015) |
| VEG | $VEG = G_N/(R_N^{0.667})*(B_N*^{0.333})$ | Guijarro *et al.* (2011)<br>Yang *et al.* (2015) |
| COM | 0.25ExG + 0.30ExGR + 0.33CIVE + 0.12VEG | Yang *et al.* (2015) |

# 6. Procedures for images acquisition

Some care must be taken in order to acquire the **correct image** of the leaves (Figures 14 and 15). First, you should only use an opaque white background to get the leaf image, as shown in the example below. The opaque white background aims to avoid excessive light being reflected from the environment, which can affects the RGB values from the object (leaves in this case). Shadows and projections of other objects on the background than not leaves also impact negativelly the measured values. Also, for the acquisition of images you should not use the flash light of the camera, as it will affect the color of the leaf, changing the real values of red, green and blue in the images. If you will acquire images in a room or on your lab, for example, take care with the kind of light into the room. Avoid take images nearby the windows or other sources of external light (Figure 16). For field-taken images, it should be considering to use a canvas sunshade, as it will reduces the influence of external light on the actual image. You need standardize the environment where you are taking your images, so try to maintain always the same procedures, including the time of the day and the distance between the sample and the device which you are using for images capture. This distance will affects the edges of the images, since some distortion effect is expected on borders, then keep your leaves always centralized. If you have a plant with large and long leaves you may cut then and disposes side by side each piece of the same leaf to acquire the image.

**Figure 14.** Example of sampling leaves for images acquisition.

**Do not take images of each piece separately.**

# 6. Procedures for images acquisition

Have a look on some images not properly acquired:

**Figure 15.** Image of multiple leaves acquired with a cellphone camera with excessive shadows on the border of the leaves.

**Figure 16.** Image of a single long leaf previously cut, acquired with a cellphone camera when room lights are negatively affecting the image.

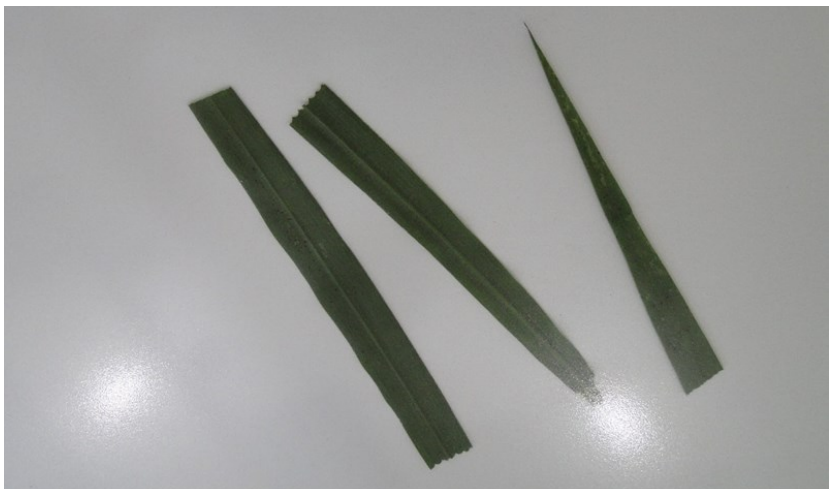

# 6. Procedures for images acquisition

Have a look on same images not properly acquired:

**Figure 17.** Image of a multiple leaves acquired with a commercial camera. Leaves are excessively rolled due to water loss.

**Figure 18.** This image can be considered a good example of the image acquisition step.

# 6. Procedures for images acquisition

Performing image collection in the field is a very important step in the process of images acquisition for further processing by the **ImageVI's software**.

In order to guarantee the accuracy of the results in the extraction of the vegetation indices from the samples, follow the 1 step by 9 step until to properly acquire the images that will be sent for processing.

1 Select an area where the leaves of the forage species will be collected, or defines a way (in zig-zag for example) to collect the leaves (Figura 19).

**Figure 19**. Images of an experimental area implanted with *Brachiaria decumbens* cv. Basilisk showing the visible differences within the paddock.

# 6. Procedures for images acquisition

2

After selecting the sampling area to be studied, select the tillers randomly and detach the leaf blade of the diagnostic leaf. The diagnostic leaf is the younger mature leaf in the tiller with visible ligule. Normally, the first fully expanded leaf is considered the diagnostic leaf, but you can also use the second fully expanded leaf (Figures 20 and 21) .

The choice of diagnostic leaves is due to the fact that, in grasses, leaf blades recently expanded, show patterns in nutrient concentrations adequate for the range of nutritional sufficiency of the species (Silveira, Nacthingall and Monteiro, 2005).

**Figure 20**. Tiller example with the youngest two leaves completely expanded with visible ligule.

**Figure 21.** Parts of a grass tiller of *Brachiaria decumbens* cv. Basilisk.

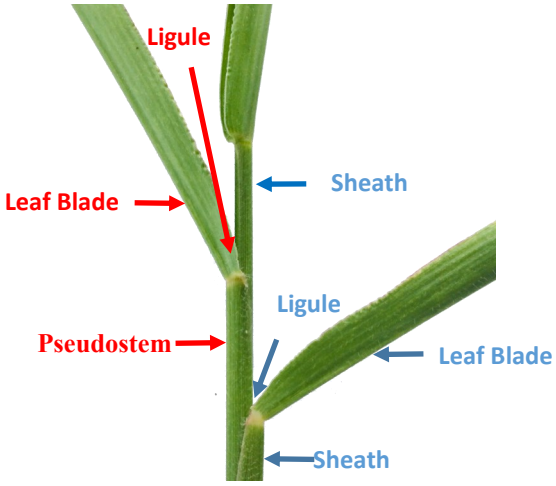

# 6. Procedures for images acquisition

3

With the assistance of pruning shears or a scissor, detach the leaf blade nearby the ligule. Make a cut just after the ligule. Remember that the ligule is is a thin outgrowth which clasps the stem at the junction of blade and sheath (Figure 22).

**Figure 22.** Collection of leaf blade using pruning shears and highlighting the boundary between the junction of blade and sheath.

# 6. Procedures for images acquisition

4 For the images acquisition through a sensor (commercial camera, scanner, smartphone or tablet cameras), it will be necessary to prepare an opaque white background base, in order to avoid excessive reflection of light.

This base of opaque white background can be implemented in the easiest way and with short investment, placing a sheet of white paper on a medium density fiber board (MDF - Medium density fiber board), as can be seen in Figure 23, or using an A4 size drawing board (Figure 24).

**Figure 23**. Image of a white background base which was improvised using an MDF tray and a white sheet of A4 paper.

**Figure 24**. A4 size drawing board in matte white color and which can also be used as a basis for image acquisition in the field.

All the basic suggestions with a white background described here in this stage are low -cost options and easy to implement. Thus, it will be possible to transport them to the field without great difficulties, as long as they respect the recommendations for standardizing the environment for acquiring images and reducing the influence of external light.

If it is not possible to acquire images in the field immediately after the collection, allocate the leaf blades in identified plastic or paper bags and keep the samples in a box with ice until they are taken to the laboratory. This procedure will decrease the temperature effects on the leaves, minimizing water loss and avoiding curling of leaves. Flatter leaves help it placement on the base during the image acquisition procedures.

# 6. Procedures for images acquisition

5 Place the leaf blades on a white base, maintaining the adaxial face upwards (Figure 25 and 26).

**Figure 25.** Two leaf blades disposed on the white background with the adaxial faced up.

**Figure 26**. Arrangement of four leaf blades on the base of a white background with the adaxial side facing up.

# 6. Procedures for images acquisition

Position the chosen sensor to perform image acquisition at approximately 23 cm height from the leaf blades (Figure 27), keeping the leaves in the center of the image (Figura 28).

**Figure 27**. Example of image acquisition using a smartphone camera, maintaining a distance of approximately 23 cm between the base and the capture sensor.

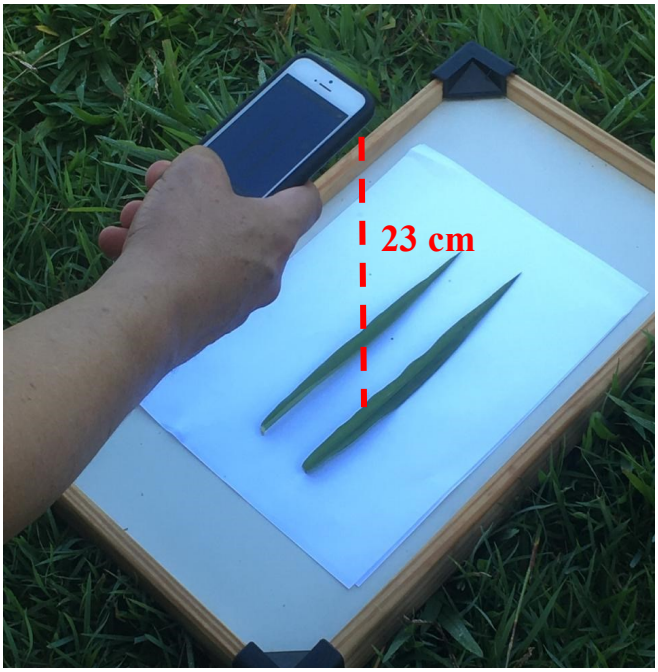


**Figure 28**. Positioning the blades in the center of the image, avoiding the capture of objects that are in the outline of the image acquisition area and that can cause noise in the image.

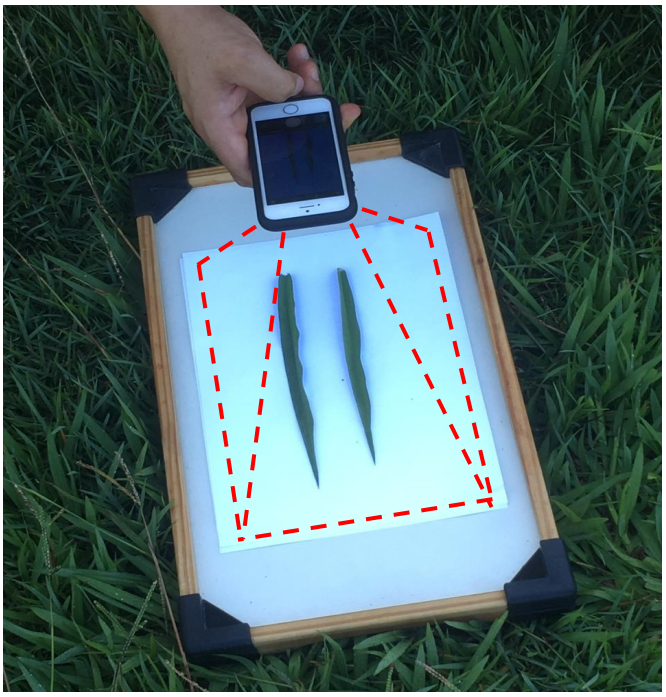

# 6. Procedures for images acquisition

Place the capture sensor at a 90 degree angle based on where the leaves are located (Figure 29).

**Figure 29.** Example of positioning at 90 degree angle between the capture sensor used and the leaves arranged on the base of a white background.

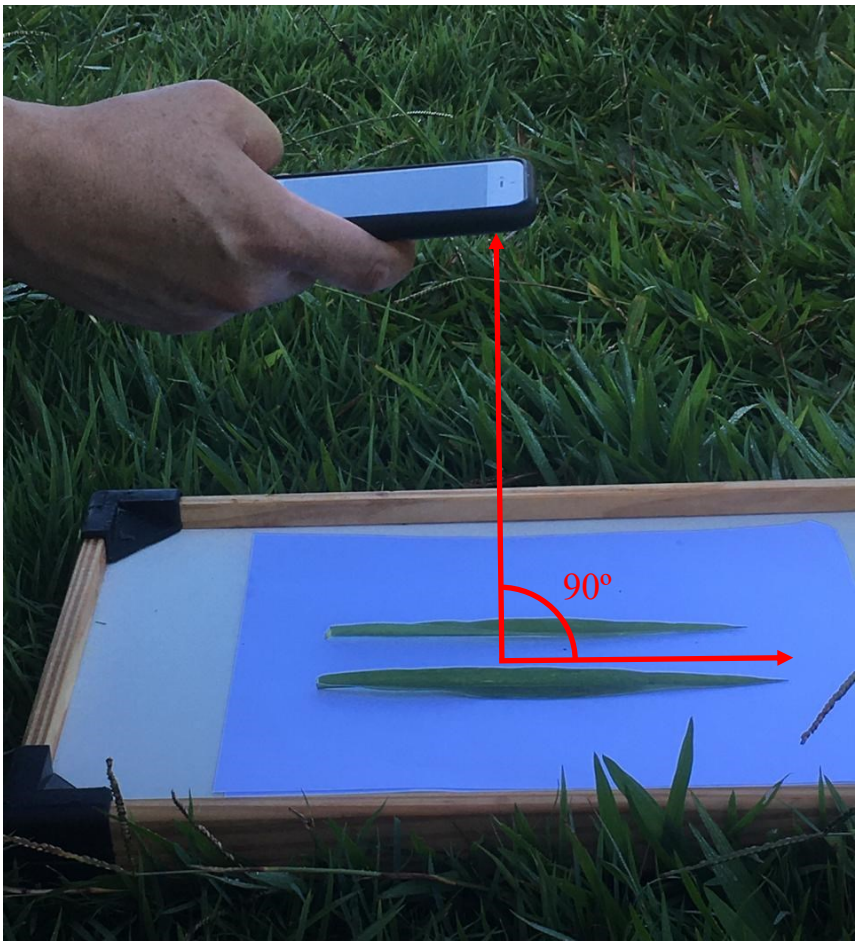


7

Finish image capture process by activating the mechanism that records the photograph according to the specifications of the sensor used.

# 6. Procedures for images acquisition

8 When capturing the image using a scanner, make the leaf blades with the adaxial part facing down (Figure 30).

**Figure 30.** Correct way of obtaining images through a scanner by arranging the leaf blades with the adaxial part facing down

# 6. Procedures for images acquisition

9 Overlay a sheet of A4 paper over the sample as shown in Figure 31. Then close the scanner cover to anchor the leaf blades and the sheet of paper (Figure 32). Press the "Scan" button of the scanner to activate the capture of the image (Figures 33), keeping the lid closed during the entire reading process.

**Figure 31**. Example of using an A4 sheet of paper over the leaf blades, in order to avoid visual noise in the image.

**Figure 32**. After overlapping the leaf blades with the A4 sheet of paper, the scanner device must be closed.

**Figure 33**. Activating the software through the scan button on the scanner device.

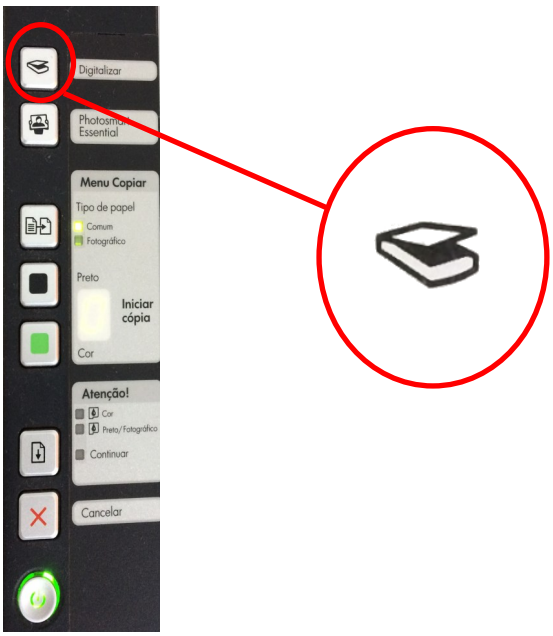

# 7. Login in the system

Once all images had been stored in your computer, in a memory stick or any external device, it will be necessary uploading them in the system. The initial step is to access the system in the following address:

http://www.mapag.com.br/softwares/imagevi/en/

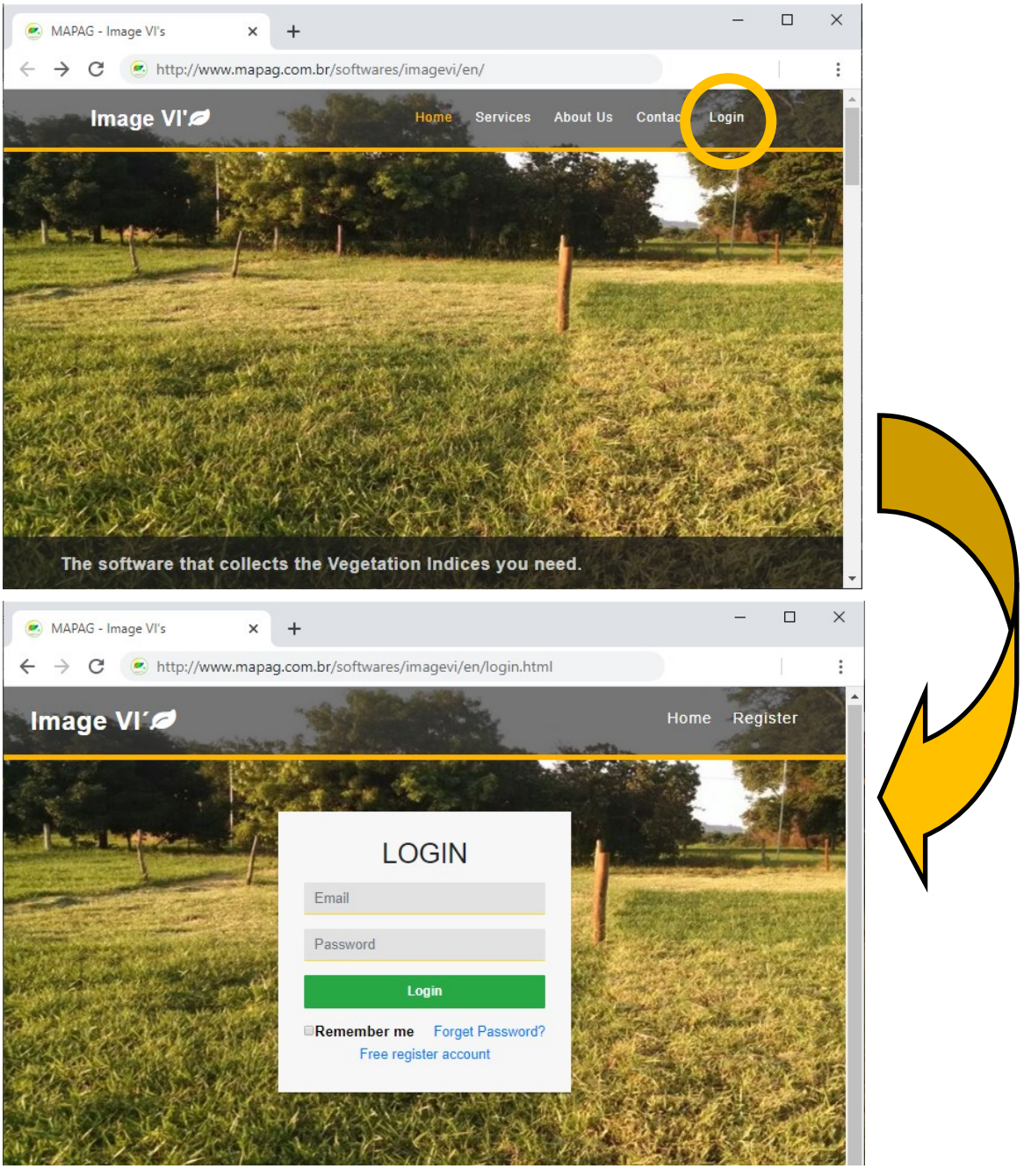

# 8. Main menu

You need to create an account, and for this you will provide your personal information. Always you need to access the software, it will be required your e-mail and password. As you created your account, you will be able to access all the funcionalities of the ImageVI's software.

In the first screen of the system, you can see the basic information contained in this USER MANUAL. You can also download the user manual by clicking the button Technical manual, in the tasks bar on the left side of your screen.

At the left side of the work area you will see the following buttons:

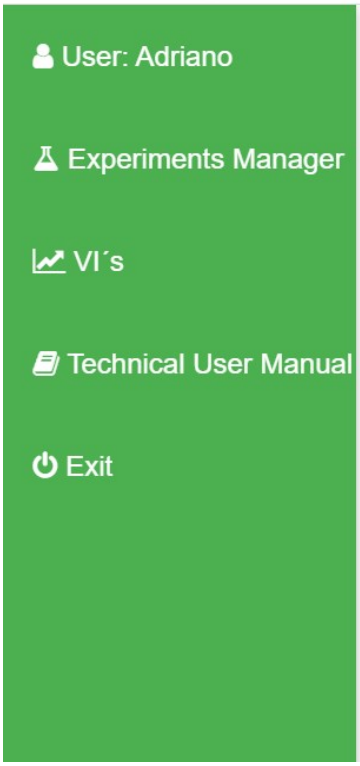


**User:** It is reffering to the name you provided when you created your account.

**Experiments Manager:** By clicking on this button you will access a new menu, where you will create folders for each experiment you want to store in the system for processing afterwards.

**VI's:** This button allows that the user has access to all the registered experiments, as well as the stored images and the generated indices.

**Technical User Manual:** Clicking on this button you can download the user manual with all the basic instructions of the system.

**Exit:** Logout of the system.

# 9. Creating an experiment

Click on the button Experiments Manager to create folders for each experiment you want to store in the system for processing afterwards.

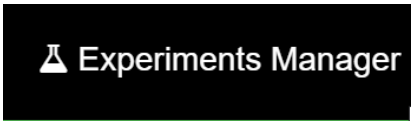


Once the 'Experiments Manager' button is clicked, you will have access to a new screen. Please, click on Create experiments.

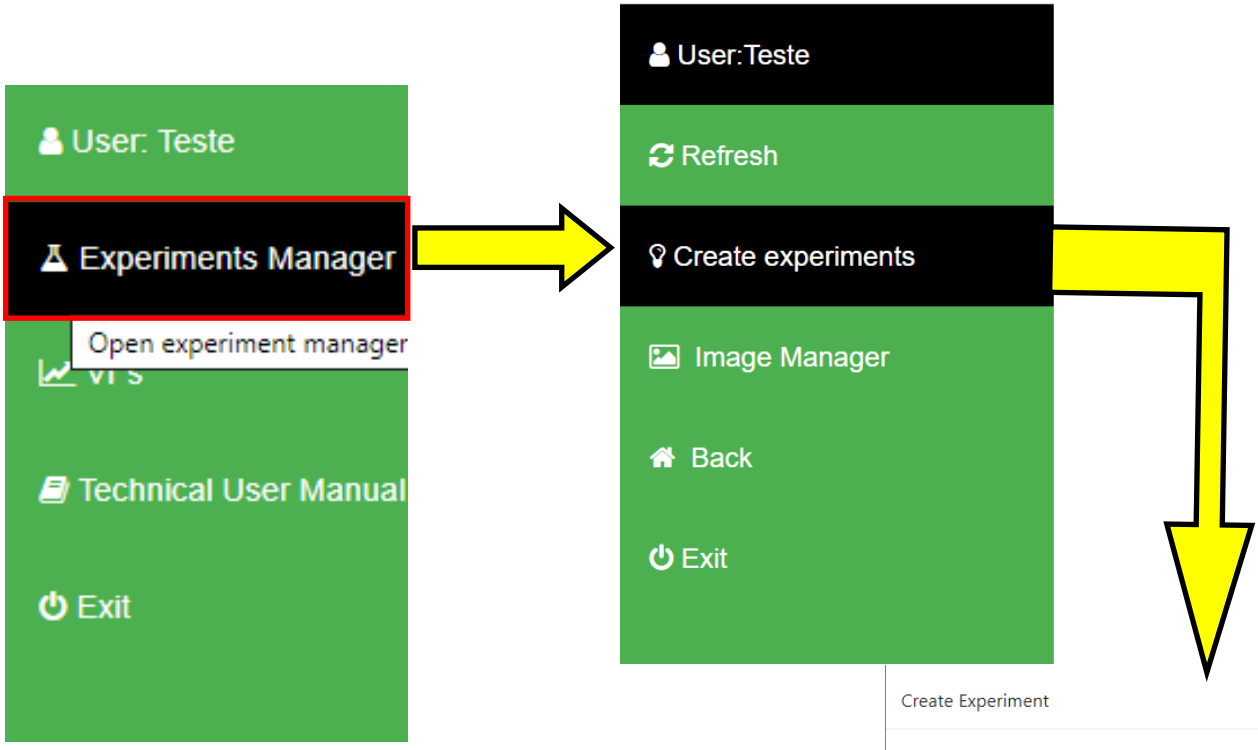


After the user clicks on **Create experiments,** a new screen for fills will open. You will provide information about the identification of the experiment, initial and final date, team and observations.

Provide the information you want to correctly identify your experiment and click on save experiment


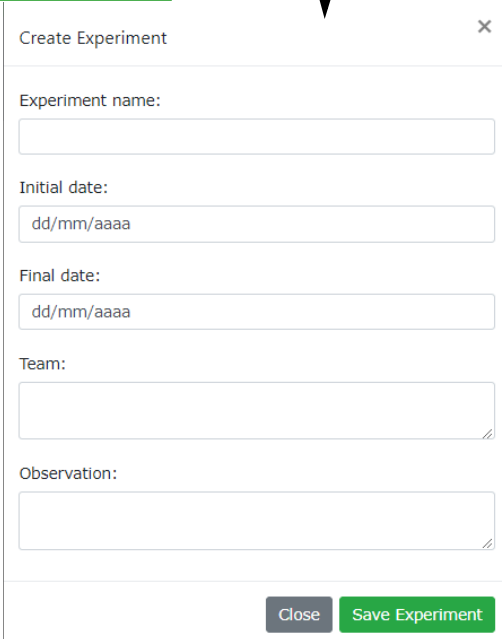

# 9. Creating an experiment

At the end of this procedure the information will be saved in the database. After registration, the experiment will be available for access and images uploading.

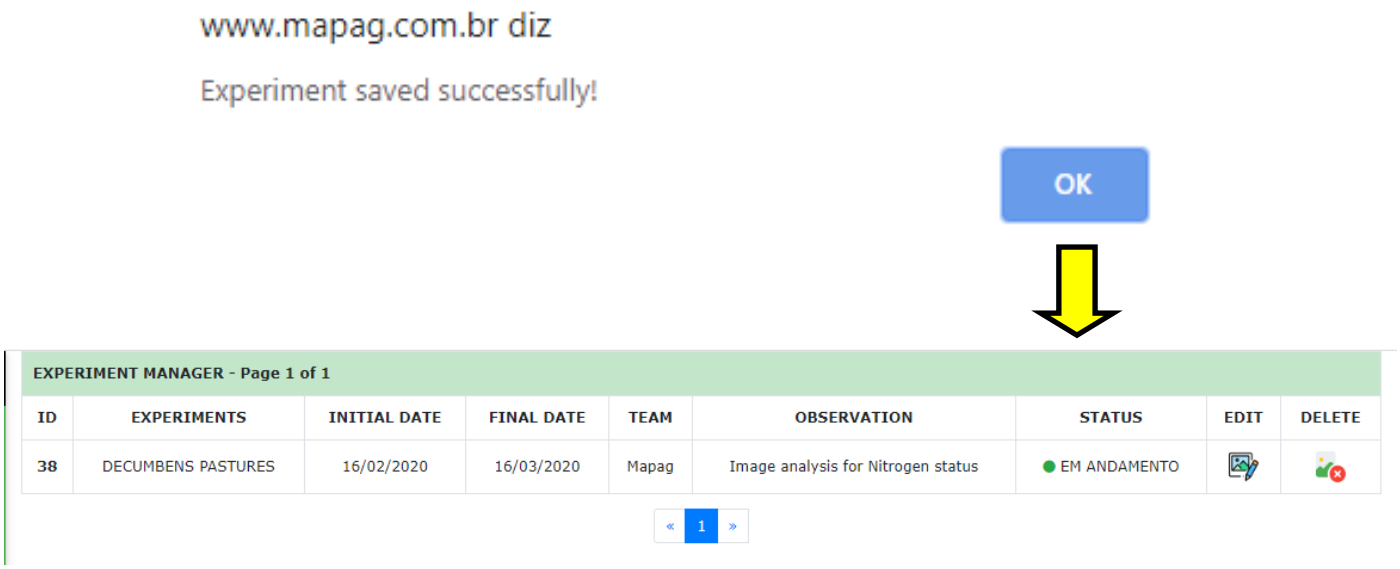


In this screen you can also change the data of the experiment or delete it by pressing the Edit or Delete button. You can also create a new experiment, according to the procedures described previously.

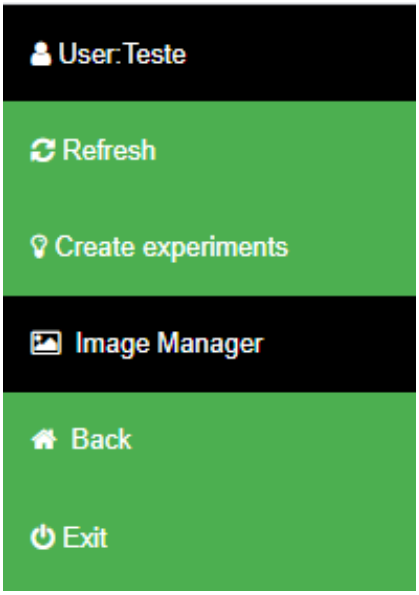


**Now, you need to upload your images into the system by pressing the button Image Manager.**

**Image Manager:** By clicking on this button you will access a new menu, which allows you to perform the upload of images.

# 10. Uploading images

To upload the images of your experiment, click on the button 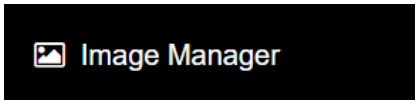


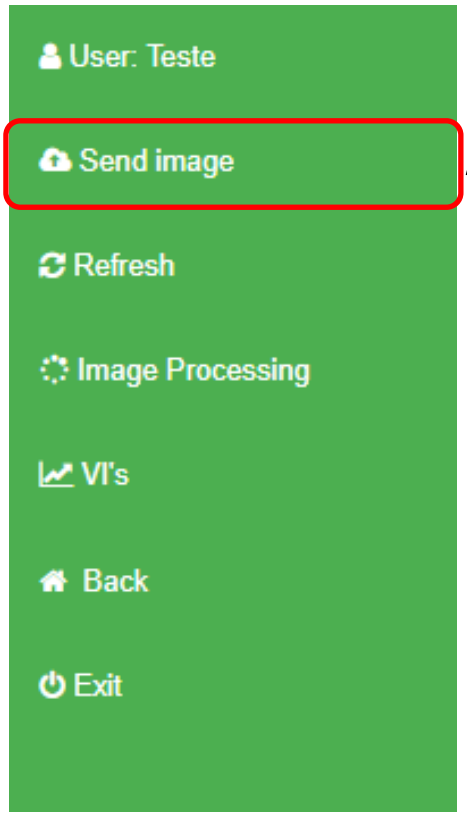


For images uploading, click the red circled button showed.

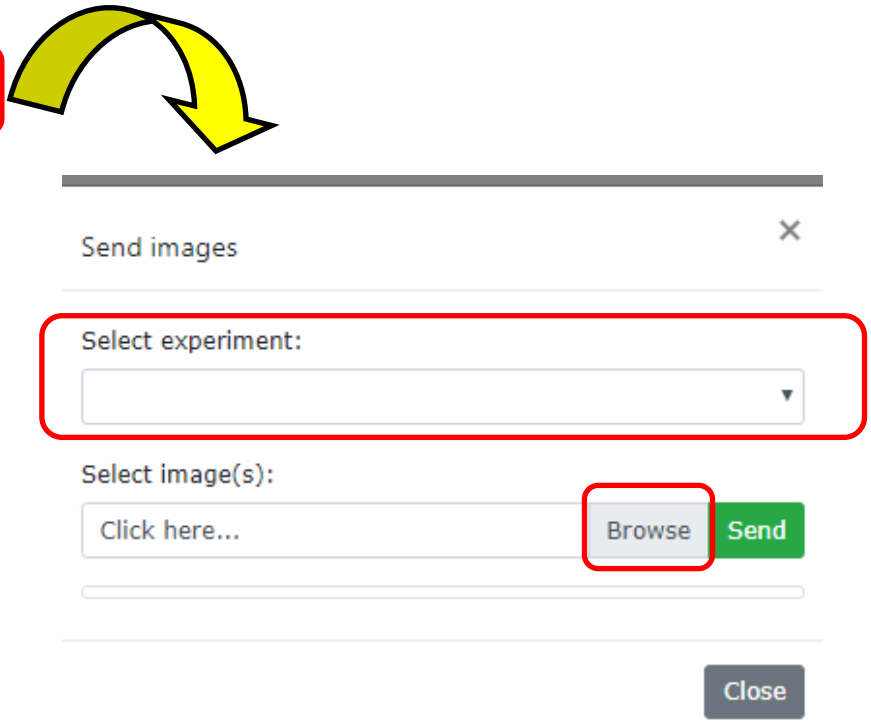


Then, select the experiment for which images are belonging to, search the images in your computer by clicking the Browse button and send it.

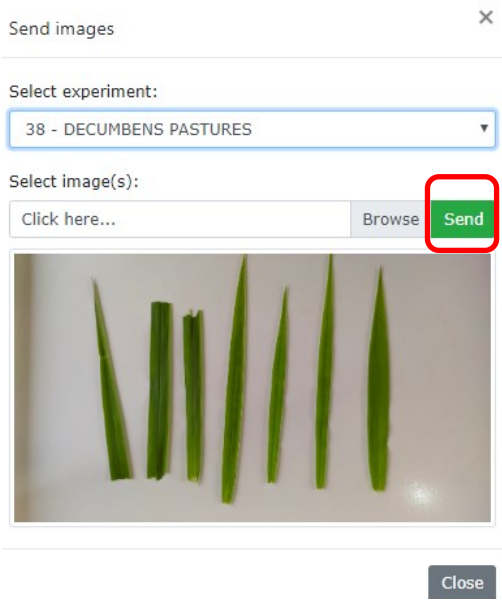


# 10. Uploading images

To send more images, you will follow the same steps described in the page 44. The system will initially upload all the images to the cloud, to later perform the processing of the same, individually or in batch (all at once), marking all the images you want to upload. After, your images will be ready for processing. Your images will be upload in the system and will appear in the work area, as is being showed in figure bellow.


In this step, and before processing, you can change the name of your image to properly identify from each experiment, plot or sample it is referring to.

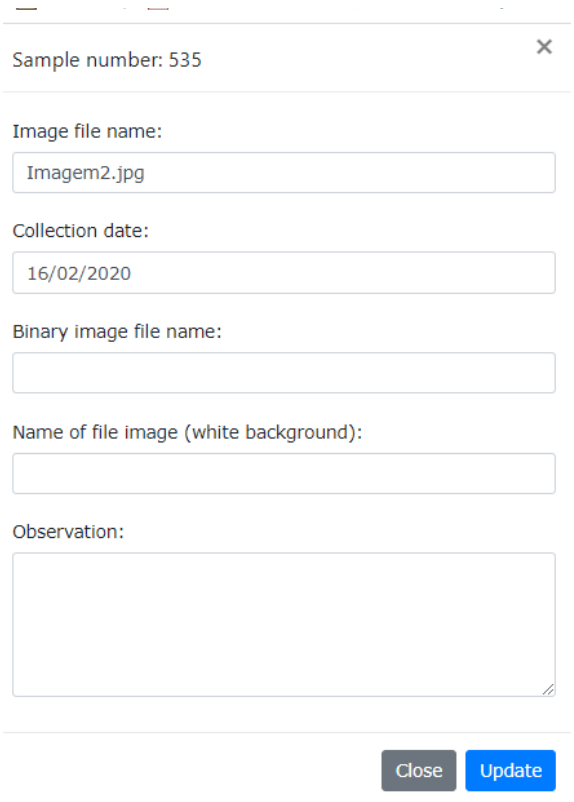


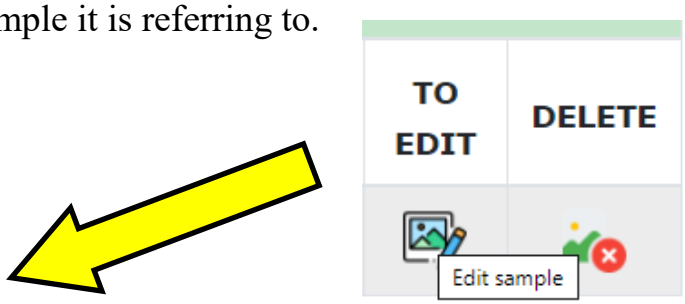


A new window will open on your work area, allowing you to change the identification (name) of the image.

After renaming the image, do not forget to click on the button UPDATE, for saving the changes.

# 11. Processing steps in the software

The steps performed by the system for image processing follow the flow chart:

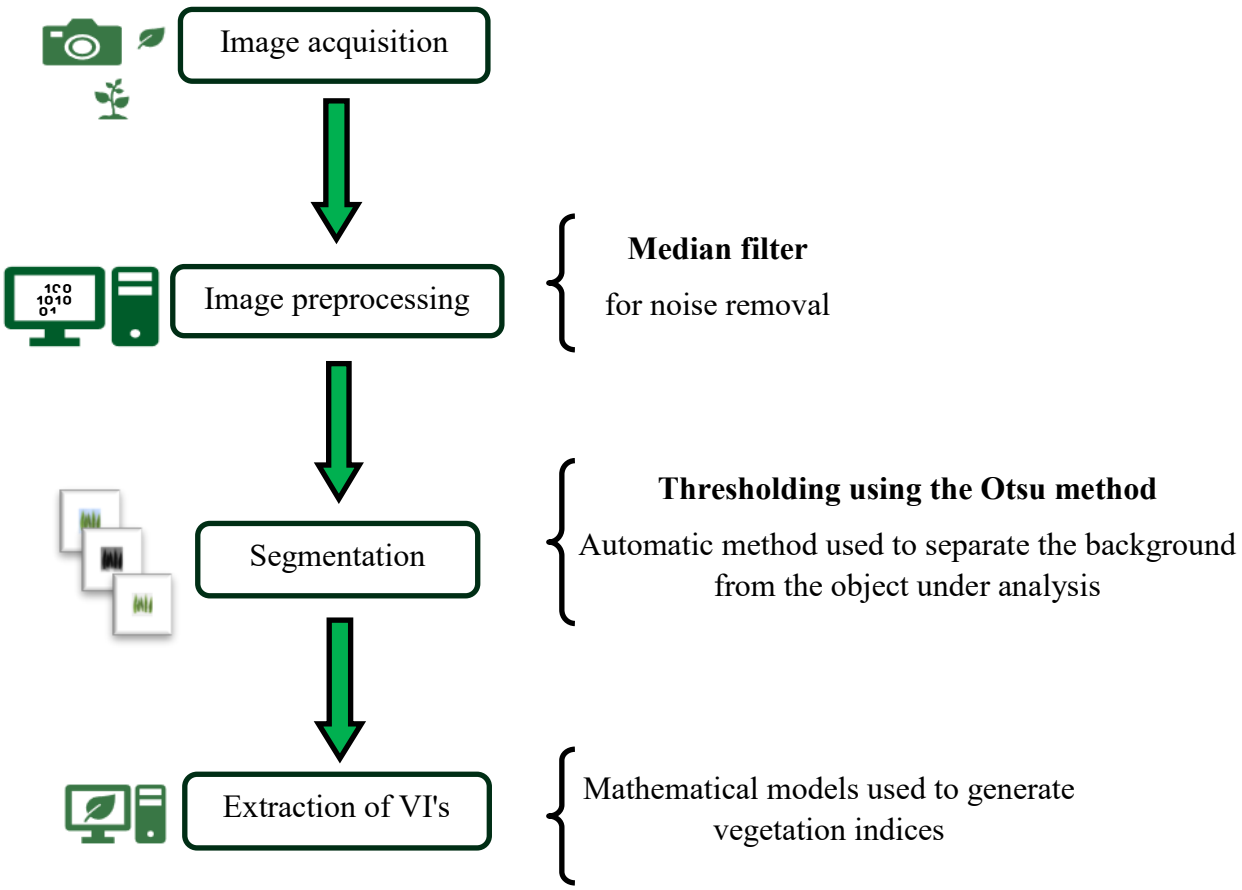

# 11. Processing steps in the software

After the images are loaded, the system will show the images stored and ready for processing. Therefore, the implemented software will process the images for the extraction of the vegetation indices. To do this, you must mark the images for processing and click on the Image Processing button.

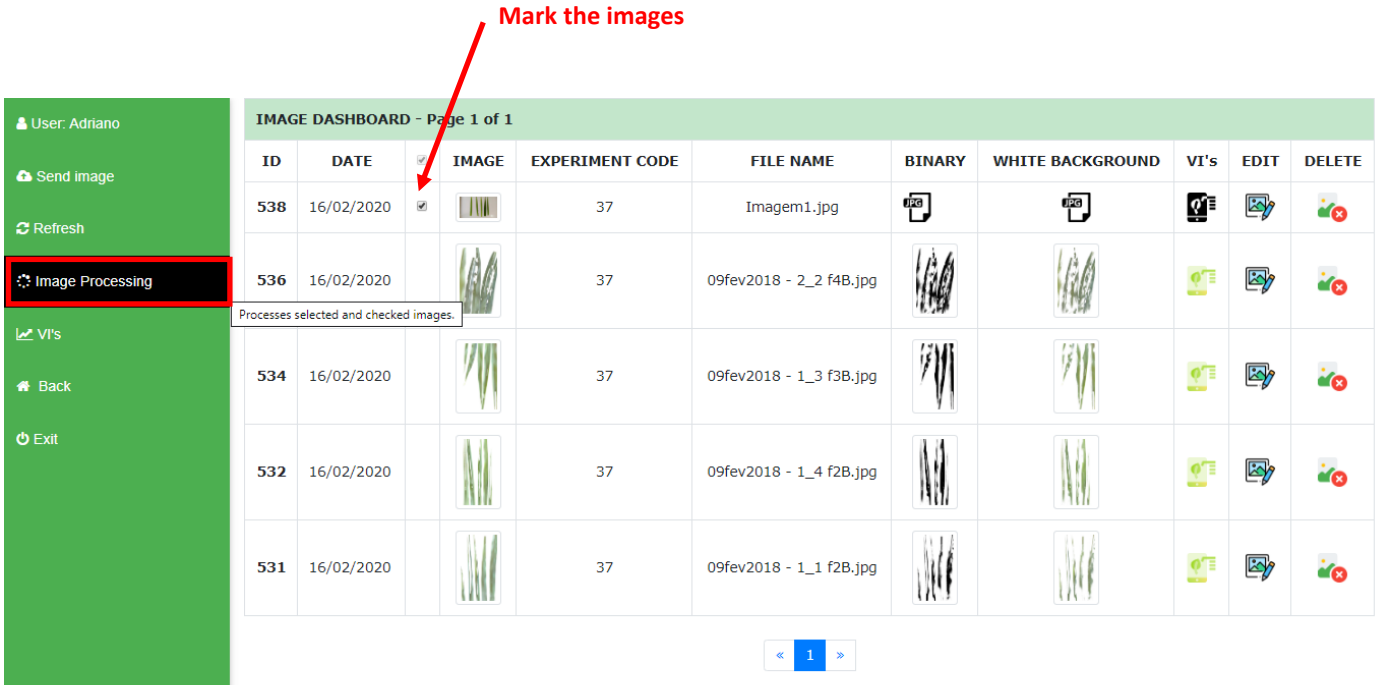


The following message will appear on the screen, "Processing ... Wait...".

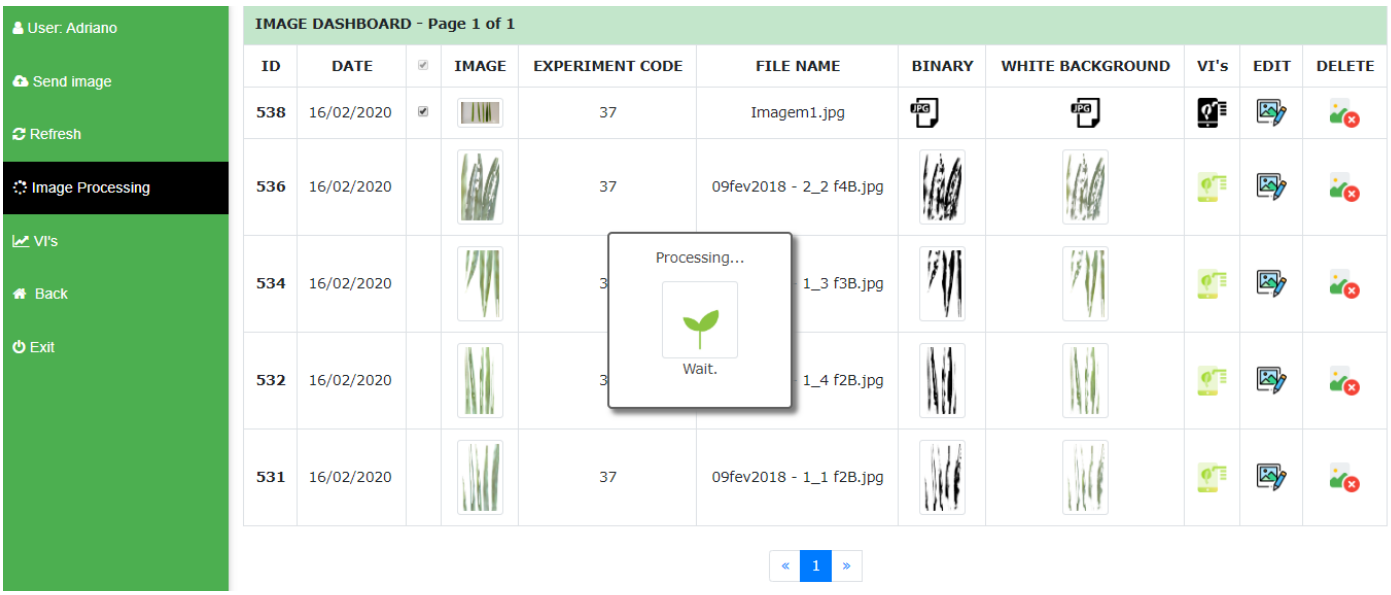

# 12. Exporting data to Excel

At the end of the processing, the system shows the generated vegetation índices individually for each image. If desired, it is possible to select an image and view it in binary

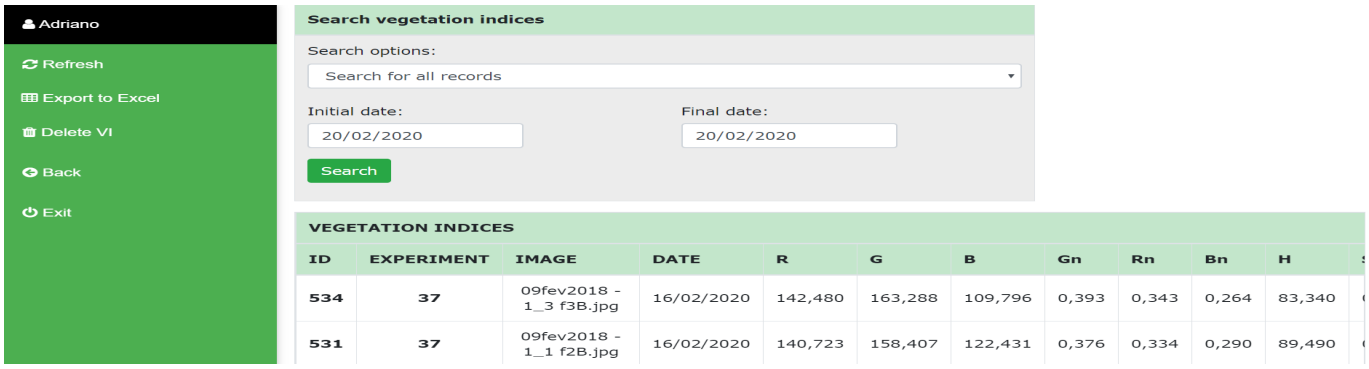


After processing, 18 vegetation indices were automatically generated, which can be exported to an Excel spreadsheet by pressing the button corresponding to Export to Excel. The system will download the Excel file for manipulation by the user.

In the next figure you will have the information regarding the processed images, you can even enter names for the images corresponding to the Binary or color White Background images, as well as having access to the indices generated by each image separately, pressing the bottons BINARY, WHITE BACKGROUND and VI's on the display screen. If you want, you can start a new experiment, following the steps presented in this manual.

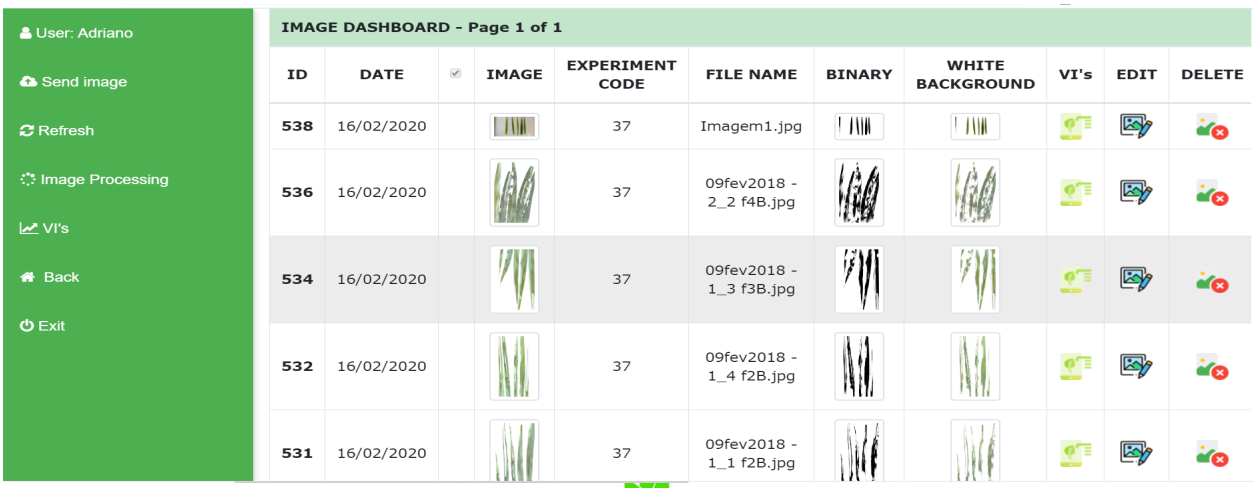

# 13. Scientific literature using VI's

In Maize (*Zea mays* L.) production, the lack of nitrogen (N) has been reported as the main constraint on cereal yields, particularly in poor tropical and subtropical soils. At the same time, the applications of N-fertilizers above the crop demand, besides increasing the production costs, can impacts negatively on the environment. Vegetation indices (VI's) derived from Red-Green-Blue (RGB) cameras have been employed for remote sensing assessment in field conditions, for quantifying leaf N concentration and correlating the VI's with grain or crop yields. According to Vergara-Diaz et al. (2016), RGB images may represent a proper alternative to spectroradiometric approaches at different levels: at the whole trial level from aerial platforms, at the plot level from ground-based measurements or even at the single leaf level, replacing leaf chlorophyll meters. Those authors observed that the vegetation indices based on RGB images demonstrated a high-throughput for the accurate prediction of several traits that are highly valuable for maize breeders and agronomists such as grain yield, leaf N concentration and the ratio of carbon to nitrogen under a wide range of N fertilization levels.

Another important finding of authors was that all VI's were better at capturing the differences in leaf N concentration than the amount of N concentration per unit leaf area proving, thus, that a possible effect of leaf thickness or density is avoided. However, a saturation point was detected at the highest N-fertilization level (160 kg/ha of N), since the VI's were not correlate with variations in leaf N concentration above that point.

# 13. Scientific literature using VI's

A corn leaf was photographed with a Canon Power Shot S51S (3264 x 2448 pixels) under fluorescent lighting (Panel A), incandescent lighting (Panel B), outside under overcast conditions (Panel C), and under full sun conditions at midday (Panel D).

Digital images were processed to determine the dark green color index (DGCI). The green and yellow disks were known colors and served as internal standards to correct for differences in lighting conditions.

**Figure 34.** Using a digital camera to assess nitrogen in corn.

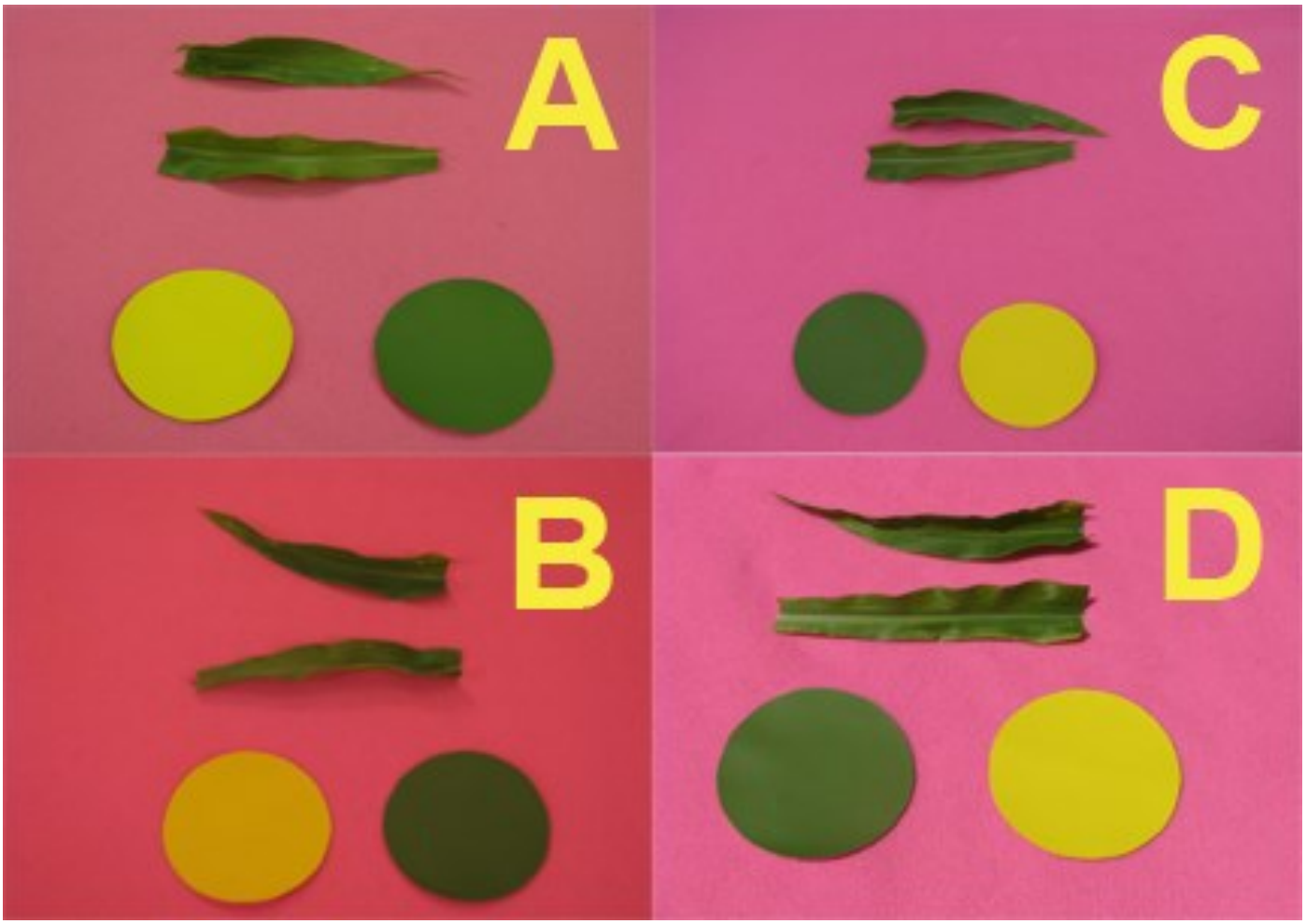


Source: Geise (2020).

# 13. Scientific literature using VI's

In rice (*Oryza sativa* L.), Zheng et al. (2018) compared three sensors (RGB sendor, color-infrared (CIR) and multispectral (MS) cameras) onboard an unmanned aerial system for the estimation of N status. When comparing the Normalized green-red difference index (G-R/G+R) and the Normalized Excess green index (2*G − R − B)/(G + R + B), for analysis of pooled datasets across all growth stages, the RGB camera performed slightly better than the same indices obtained with a multispectral camera for estimating leaf nitrogen and plant nitrogen accumulation.

**Figure 35:** Mobile application for estimating nitrogen fertilization rates in rice.

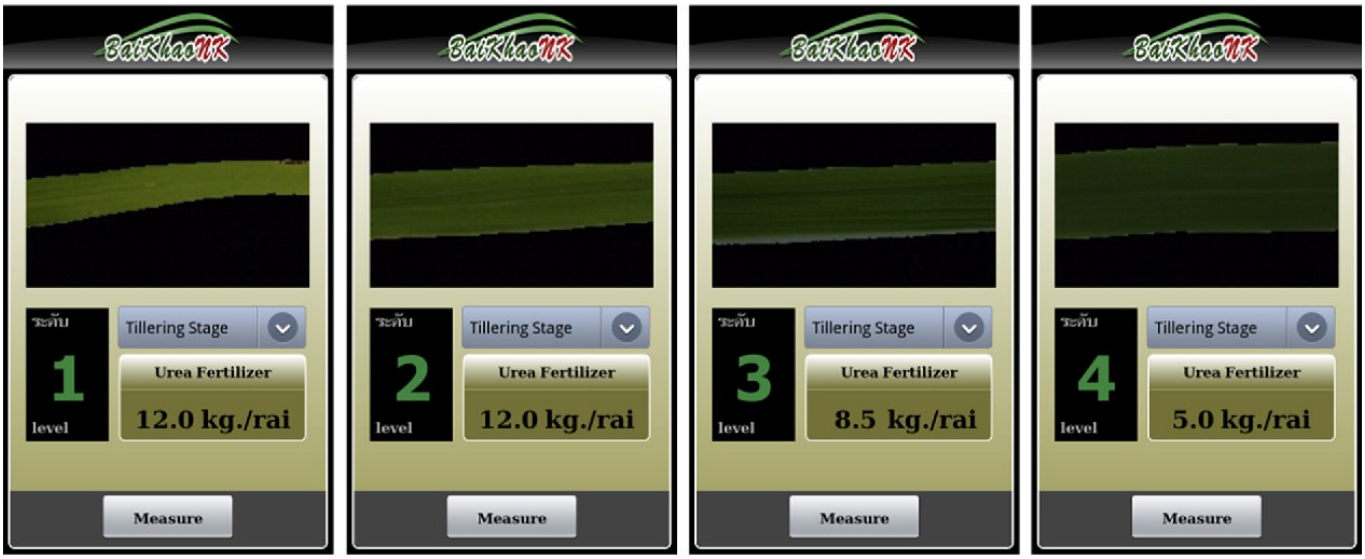


Source: Intaravanne and Sumriddetchkajorn (2012).

Caturegli et al. (2020) used the Dark Green Color Index (DGCI), proposed by Karcher and Richardson (2003), as an alternative to the spectroradiometric approaches that involve the use of NDVI from aerial platforms and from ground-based measurements to estimate leaf nitrogen content and other parameters of turf quality on mature turfgrass stands of the warm-season bermudagrass hybrid and in the cool-season tall fescue (*Schedonorus phoenix* [Scop.] (Scopoli) Holub) cv 'Grande'. DGCI was significantly correlated with color intensity, turfgrass quality and plant water content (PWC) with correlation values ranging between 0.83 and 0.95 for color intensity, 0.84 and 0.92 for turfgrass quality and 0.84 and 0.98 for PWC for bermudagrass and tall fescue, respectively.

# 13. Scientific literature using VI's

However, authors highlighted that differences in camera quality, settings and lighting conditions could affect DGCI and limit their utility in diagnosing N deficiencies. Furthermore, disease, water status, nutritional deficiencies other than N, or different uniformity, texture and growth habit may affect greenness regardless of N status (Caturegli et al., 2020) .

Image analysis has also been widely applied by using smartphones (Confalonieri et al., 2015; Delgado et al., 2013; Mohan and Gupta, 2019 and Rigon et al., 2016). According to Hernández, Marty and Guerrero et al. (2017), the use of smartphone had created opportunities for diagnostic, prognostic, detection, quantification, monitoring, control or make mobile applications, because it could be used to run routine test, does not need trained personal, its portability and is considered as a low cost device.

Wang et al. (2018) developed an Android platform to estimate nitrogen contents in cotton leaves. The VI's used were the average values of R, G and B, (R-means, G-means, B-means, red standardized mean RN = R /(R + G + B), green standardized mean GN = G /(R + G + B) and blue standardized mean BN = B /(R + G + B), hue (H), saturation (S), brightness (B or V). The method of image processing of cotton leaves was implemented in Java, including image denoising, color correction, image segmentation, extraction of color feature information of leaf area, and the prediction model of nitrogen content based on an improved backpropagation (BP) algorithm. The whole system includes the modules of taking images, selecting images, image denoising, color correction, image segmentation and calculation of nitrogen content.

**Figure 36:** Mobile application screen developed by Wang et al. (2018) for nitrogen nutrition diagnosis in cotton leaves. (Available in: http://www.jcomputers.us/vol13/jcp1311-04.pdf )

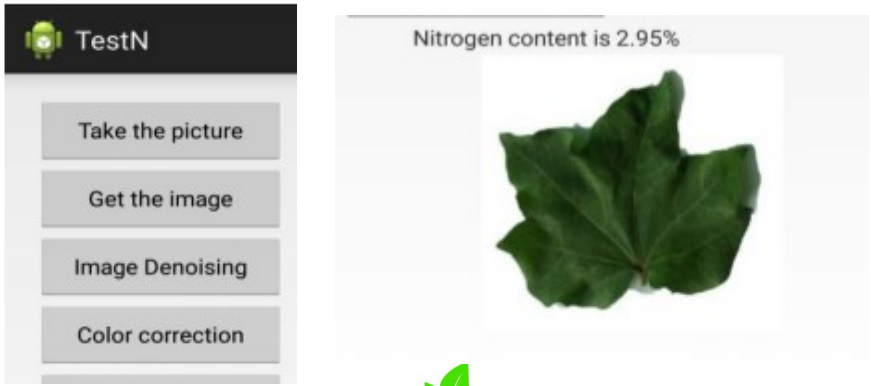

# 14. References

ANNADURAI, S.; SHANMUGALAKSHMI, R. **Fundamentals of digital image processing**. 1th ed. New Delhi: Pearson Education India, 2007.

**As diferenças entre o MYK x RGB**. Available in: <https://blog.expanssiva.com.br/as-diferencas-de-cmyk-x-rgb/ >. Access in: 03 fev. 2020.

BARBOSA, J. *et al.* Uso de imagens digitais obtidas com câmeras para analisar plantas. **Revista de Ciências Agrárias**, v. 39, n. 1, p. 15–24, mar. 2016.

BAREJA, B. G. **What is light? This question is relevant in reviewing photosynthesis and plant growth and development** (2012). Available in: <https://www.cropsreview.com/what-is-light.html>. Access in: 17 jan. 2020.

BANNARI, A. et al. A review of vegetation indices. **Remote sensing reviews**, v. 13, n. 1-2, p. 95-120, 1995.

BEAR, J. H. (2019). **The HSV Color Model in Graphic Design**. Available in: <https://www.lifewire.com/what-is-hsv-in-design-1078068>. Access in: 13 jan. 2020.

BENIAICH, A. *et al.* Determination of vegetation cover index under different soil management systems of cover plants by using an unmanned aerial vehicle with an onboard digital photographic camera. **Semina: Ciências Agrárias**, v. 40, n. 1, p. 49-66, feb. 2019.

BURGOS-ARTIZZU, X. P. *et al.* Real-time image processing for crop/weed discrimination in maize fields. **Computers and Electronics in Agriculture**, v. 75, n. 2, p. 337–346, feb. 2011.

BUSCAGLIA, H. J.; VARCO, J. J. Early detection of cotton leaf nitrogen status using leaf reflectance. **Journal of Plant Nutrition**, v. 25, n. 9, p. 2067–2067, sept. 2002.

CATUREGLI, L. *et al.* Normalized Difference Vegetation Index versus Dark Green Colour Index to estimate nitrogen status on bermudagrass hybrid and tall fescue. **International Journal of Remote Sensing**, v. 41, n. 2, p. 455–470, jan. 2020.

CONFALONIERI, R. *et al.* Improving in vivo plant nitrogen content estimates from digital images: Trueness and precision of a new approach as compared to other methods and commercial devices. **Biosystems Engineering**, v. 135, p. 21–30, july. 2015.

CUNHA, A. L. Introdução à visão computacional. Available in:<https://www.stt.eesc.usp.br/andre/palestras/CEFET-MG/01_Intro.html>. Access in: 10 jan. 2020.

DAVIDSON, M. *et al.* Mapping photosynthesis from space - A new vegetation-fluorescence technique. **Esa Bulletin-European Space Agency**, v. 116, p. 34–37, 2003. Available in: <Available in: http://www.esa.int/esapub/bulletin/bullet116/chapter4_bul116.pdf >. Access in: 13 jan. 2020.

DELGADO, J. A.; KOWALSKI, K.; TEBBE, C. The first Nitrogen Index app for mobile devices: Using portable technology for smart agricultural management. **Computers and Electronics in Agriculture**, v. 91, p. 121–123, feb. 2013.

DEKEL, G. RGB and CMYK Colour systems. Available in: <http://www.poeticmind.co.uk/research/rgb-cmyk-colour-systems/>. Access in: 10 jan. 2020.

EL-AZAZY, A. Inspect the potential of using leaf image analysis procedure in estimating nitrogen status in citrus leaves. **Middle East Journal of Agriculture Research**, v. 07, n. 03, p. 1059–1071, 2018.

MEYER, G. E. *et al.* Textural imaging and discriminant analysis for distinguishingweeds for spot spraying. **Transactions of the ASAE**, v. 41, n. 4, p. 1189–1197, jan. 1998.

GIESE, J. **Using a digital camera to assess nitrogen in corn**. Available in: <https://www.certifiedcropadviser.org/science-news/using-digital-camera-assess-nitrogen-corn>. Acesso em: 10 feb. 2020.

GITELSON, A. A. *et al.* Novel algorithms for remote estimation of vegetation fraction. **Remote Sensing of Environment**, v. 80, n. 1, p. 76–87, apr. 2002.

___. Remote estimation of crop fractional vegetation cover: the use of noise equivalent as an indicator of performance of vegetation indices. **International Journal of Remote Sensing**, v. 34, n. 17, p. 6054–6066, sept. 2013.

GONZALEZ, R. C.; WOODS, R. E. **Digital image processing**. 3th ed. Upper Saddle River: Pearson Prentice Hall, 2008.

GUIJARRO, M. *et al.* Automatic segmentation of relevant textures in agricultural images. **Computers and Electronics in Agriculture**, v. 75, n. 1, p. 75–83, jan. 2011.

HERNÁNDEZ, D. B.; MARTY, J. L.; GUERRERO, R. M. Smartphone as a portable detector, analytical device, or instrument Interface. *In*: **Smartphones from an Applied Research Perspective**. [s.l.] InTech, 2017.

**Healthy crop**. Available in: <https://midopt.com/healthy-crop/ >. Access in: 13 feb. 2020.

**How does light frequency affect the rate of photosynthesis?** Available in: <https://socratic.org/questions/how-does-light-frequency-affect-the-rate-of-photosynthesis>. Access in: 13 feb. 2020.

**Hue, Value, Saturation**. Available in: <http://learn.leighcotnoir.com/artspeak/elements-color/hue-value-saturation/>. Access in: 10 feb. 2020.

INTARAVANNE, Y.; SUMRIDDETCHKAJORN, S. **BaiKhao (rice leaf) app: a mobile device-based application in analyzing the color level of the rice leaf for nitrogen estimation**. (T. Shimura et al., Eds.). 30 nov. 2012. Available in: <http://proceedings.spiedigitallibrary.org/proceeding.aspx?doi=10.1117/12.2001120>. Access in: 17 jan. 2020.

KARCHER, D. E.; RICHARDSON, M. D. Quantifying turfgrass color using digital image analysis. **Crop Science**, v. 43, n. 3, p. 943, 2003.

KATAOKA, T. *et al.* **Crop growth estimation system using machine vision.** Proceedings 2003 IEEE/ASME International Conference on Advanced Intelligent Mechatronics (AIM 2003). **Anais**...IEEE, [s.d.] Available in: <http://ieeexplore.ieee.org/document/1225492/>. Access in: 13 fev. 2020.

**Light and photosynthetic pigments**. Available in: <https://www.khanacademy.org/science/biology/photosynthesis-in-plants/the-light-dependent-reactions-of-photosynthesis/a/light-and-photosynthetic-pigments>. Access in: 10 feb. 2020.

MANCIN, W. R. **Desenvolvimento de software de processamento digital de imagens para análise do status nutricional de nitrogênio em Brachiaria brizantha cv. Xaraés utilizando rede neural artificial**. 2019. 60f. Dissertação (Mestrado em Gestão e Inovação na Indústria Animal) - Faculdade de Zootecnia e Engenharia de Alimentos, Universidade de São Paulo, Pirassununga, 2020.

MASONER, L. A. **Brief History of Photography and the Camera**. Available in: <https://www.https://www.thesprucecrafts.com/brief-history-of-photography-2688527>. Access in: 13 jan. 2020.

MATA-DONJUAN, G. F. *et al*. Use of improved hue, luminance and saturation (IHLS) color space in the estimation of Nitrogen on tomato seedlings (*Lycopersicon esculentum*). **Scientific Research and Essays**, v. 7, n. 27, july. 2012.

MEYER, G. E.; CAMARGO NETO, J. Verification of color vegetation indices for automated crop imaging applications. **Computers and Electronics in Agriculture**, v. 63, n. 2, p. 282–293, oct. 2008.

MEYER, G.E. et al. Textural imaging and discriminant analysis for distinguishing weeds for spot spraying. **Transactions of the ASAE**, v 41, p. 1189–1197, 1998.

MOHAN, P.; GUPTA, S. Intelligent image analysis for retrieval of leaf chlorophyll content of rice from digital images of smartphone under natural light. **Photosynthetica**, v. 57, n. 2, p. 388–398, may 2019.

**Painting Cartoon PNG - Transparent PNG Image**. Available in: <https://www.subpng.com/png-b2601i/download.html>. Access in: 10 jan. 2020.

PONZONI, F. J.; SHIMABUKURO, Y. E.; KUPLICH, T. M. **Sensoriamento remoto da vegetação**. 2º ed. São Paulo: Oficina de Textos, 2012.

RELJIC, D. **Cartoon (2018)**. Available in: <https://www.https://www.boldbusiness.com/digital/facial-recognition-cows-can-change-agriculture/>. Access in: 10 jan. 2020.

RIGON, J. P. G. *et al.* A novel method for the estimation of soybean chlorophyll content using a smartphone and image analysis. **Photosynthetica**, v. 54, n. 4, p. 559–566, dec. 2016.

RORIE, R. L. *et al.* The assessment of leaf nitrogen in corn from digital images. **Crop Science**, v. 51, n. 5, p. 2174, 2011.

SABERIOON, M. M. *et al.* Assessment of rice leaf chlorophyll content using visible bands at different growth stages at both the leaf and canopy scale. **International Journal of Applied Earth Observation and Geoinformation**, v. 32, p. 35–45, oct. 2014.

SILVEIRA, C. P.; NACHTIGALL, G. R.; MONTEIRO, F. A. Norms for the diagnosis and recommendation integrated system for signal grass. Scientia Agricola, v. 62, n. 6, p. 513–519, dec. 2005.

SIMS, D. A.; GAMON, J. A. Relationships between leaf pigment content and spectral reflectance across a wide range of species, leaf structures and developmental stages. **Remote Sensing of Environment**, v. 81, n. 2–3, p. 337–354, aug. 2002.

SRIDEVY, S. *et al.* Nitrogen and potassium deficiency identification in maize by image mining, spectral and true colour response. **Indian Journal of Plant Physiology**, v. 23, n. 1, p. 91–99, mar. 2018.

**The Complete History of Studio Photography – Timeline**. Available in: <https://www.https://www.misterlocation.com/blog/history-of-studio-photography-timeline/>. Access in: 13 feb. 2020.

**The light spectrum (First Generation LED Light Spectrums)**. Available in: <https://ledgrowlightsguides.com/full-spectrum-led-grow-light/>. Access in: 01 fev. 2020.

VERGARA-DÍAZ, O. *et al.* A novel remote sensing approach for prediction of maize yield under different conditions of nitrogen fertilization. **Frontiers in Plant Science**, v. 7, may 2016.

WANG, Y. *et al.* Estimating rice chlorophyll content and leaf nitrogen concentration with a digital still color camera under natural light. **Plant Methods**, v. 10, n. 1, p. 36, 2014.

WANG, Y. *et al.* Study on Monitoring methods of nitrogen nutrition in cotton leaves based on android platform. **Journal of Computers**, v. 13, n. 11, p. 1272–1278, 2018.

WOEBBECKE, D. M. et al. Color indices for weed identification under various soil, residue, and lighting conditions. **Transactions of the AAmerican Society of Agricultural Engineers**, v. 38, n. 1, p. 259–269, 1995.

YANG, W. *et al.* Greenness identification based on HSV decision tree. **Information Processing in Agriculture**, v. 2, n. 3–4, p. 149–160, out. 2015.

YUAN, Y. *et al.* Diagnosis of nitrogen nutrition of rice based on image processing of visible light. IEEE International Conference on Functional-Structural Plant Growth Modeling, Simulation, Visualization and Applications (FSPMA). **Anais**...IEEE, nov. 2016. Available in: <http://ieeexplore.ieee.org/document/7818311/>. Access in: 08 jan. 2020.

ZHENG, H. *et al.* Evaluation of RGB, color-infrared and multispectral images acquired from unmanned aerial systems for the estimation of nitrogen accumulation in rice. **Remote Sensing**, v. 10, n. 6, p. 824, may 2018.

# 14. About the authors

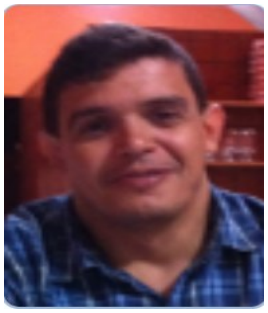

**Adriano Aparecido Virgílio:** Professor I at the Paula Souza State Center for Technological Education. Master's student in Management and Innovation in the Animal Industry (Professional Master's Degree) (FZEA/USP), Bachelor in Systems Analysis and Development from the Anhanguera University of São Paulo and Specialization in Informatics in Education from FAVENI - Faculty Venda Nova do Imigrante.
E-mail: adrianovirgilio@usp.br

**Adriano Rogério Bruno Tech:** Professor in the Department of Basic Sciences (ZAB), Faculty of Animal Science and Food Engineering (FZEA), University of São Paulo (USP). PhD in Animal Science (FZEA/USP), Master in Information System from the Pontifical Catholic University of Campinas (PUCCAMP /SP) and Bachelor of Engineering Surveying (FEAP /SP). Lecturer in the courses of Animal Science, Food Engineering, Biosystems Engineering and Lecturer / Advisor in the Postgraduate Programs in Management and Innovation in the Animal Industry (Professional Master's Degree) (FZEA/USP) and in the Environmental Engineering Sciences Program (EESC/USP). Fellow Productivity in Technological Development and Innovative Extension (CNPq - DT 2). Coordinator of the Research Group on Environment Monitoring, Large Crops and Pastures (CNPq).
E-mail: adriano.tech@usp.br

**Lilian Elgalise Techio Pereira:** Professor in the Department of Animal Science (ZAZ) at the Faculty of Animal Science and Food Engineering (FZEA) at the University of São Paulo (USP). PhD in Animal Science and Pasture (ESALQ/USP), Master in Animal Science and Pasture (ESALQ / USP) and Bachelor of Animal Science (UFSM). Lecturer in the Animal Science and Veterinary Medicine courses and Lecturer / Advisor in the Postgraduate Programs in Management and Innovation in the Animal Industry (Professional Master's Degree) (FZEA/USP) and in the Animal Science Program (FZEA/USP). Coordinator of the Research Group on Environment Monitoring, Large Crops and Pastures (CNPq).
E-mail: ltechio@usp.br


**ISBN 978-65-87023-00-7 (e-book)**